Cell Tissue Res (2013) 354:793–812
DOI 10.1007/s00441-013-1716-5

REGULAR ARTICLE

New facets of keratin K77: interspecies variations of expression and different intracellular location in embryonic and adult skin of humans and mice

Lutz Langbein · Julia Reichelt · Leopold Eckhart · Silke Praetzel-Wunder · Walter Kittstein · Nikolaus Gassler · Juergen Schweizer

Received: 23 April 2013 / Accepted: 19 July 2013 / Published online: 22 September 2013

Abstract The differential expression of keratins is central to the formation of various epithelia and their appendages. Structurally, the type II keratin K77 is closely related to K1, the prototypical type II keratin of the suprabasal epidermis. Here, we perform a developmental study on K77 expression in human and murine skin. In both species, K77 is expressed in the suprabasal fetal epidermis. While K77 appears after K1 in the human epidermis, the opposite is true for the murine tissue. This species-specific pattern of expression is also found in conventional and organotypic cultures of human and murine keratinocytes. Ultrastructure investigation shows that, in contrast to K77 intermediate filaments of mice, those of the human ortholog are not attached to desmosomes. After birth, K77 disappears without deleterious consequences from human epidermis while it is maintained in the adult mouse epidermis, where its presence has so far gone unnoticed. After targeted *Krt1* gene deletion in mice, K77 is normally expressed but fails to functionally replace K1. Besides the epidermis, both human and mouse K77 are present in luminal duct cells of eccrine sweat glands. The demonstration of a K77 ortholog in platypus but not in non-mammalian vertebrates identifies K77 as an evolutionarily ancient component of the mammalian integument that has evolved different patterns of intracellular distribution and adult tissue expression in primates.

Keywords Intermediate filaments · Cytoskeleton · Differentiation · Eccrine sweat glands · Development

Electronic supplementary material The online version of this article (doi:10.1007/s00441-013-1716-5) contains supplementary material, which is available to authorized users.

L. Langbein (✉) · S. Praetzel-Wunder
Genetics of Skin Carcinogenesis, A110, German Cancer Research Center, Im Neuenheimer Feld 280, 69120 Heidelberg, Germany
e-mail: langbein@dkfz.de

W. Kittstein · J. Schweizer
German Cancer Research Center, Heidelberg, Germany

J. Reichelt
Institute of Cellular Medicine, Dermatological Sciences, Newcastle University, Newcastle upon Tyne, UK

L. Eckhart
Department of Dermatology, Medical University of Vienna, Vienna, Austria

N. Gassler
Institute of Pathology, RWTH Aachen University, Aachen, Germany

Introduction

The human keratin gene family comprises 54 members and at least one functional alternative splice variant (Schweizer et al. 2006; Langbein et al. 2010a). For each of these keratins, the exact location within the type I (chromosome 17) and type II (chromosome 12) gene clusters, as well as their gene and protein sequences are known (Hesse et al. 2004; Rogers et al. 2004, 2005; Schweizer et al. 2006). With the exception of the type I keratins K23 and K24 and the type II keratins K78 and K79, the expression profiles of the individual keratins in the different types of normal and pathologically altered human epithelia have been studied extensively (Moll et al. 2008). Based on their expression profiles, the keratins of all epithelia (including hard keratinizing skin appendages) can be subdivided into 37 epithelial keratins and 17 hair keratins. The hair follicle contains a particularly high diversity of keratins with 9 epithelial keratins being specifically expressed in the concentric epithelial layers encasing the hair-forming compartment, which in turn contains 16 hair keratins (Langbein and Schweizer 2005, 2013; Langbein et al. 2006, 2007, 2010a, b).

These studies also showed that distinct type II/type I keratin pairs are specifically and differentially expressed in the various epithelia. Thus, keratin pair K5/K14 is typical for the basal, proliferative cell layer of stratified epithelia, while the pairs K1/K10, K4/K13 and K3/K12 are representative of differentiating compartments of cornified and non-cornified squamous epithelia, as well as the corneal epithelium, respectively. In addition, the integrity of non-stratified simple epithelia relies essentially on keratins K8/K18 (Moll et al. 2008). Frequently, these "basic" keratins are supplemented by "accessory" keratins such as the epidermal keratins K2 and K9, which distinguish specific epidermal regions, the keratin pair K6/K16, which marks "activated states" in hyperproliferating and/or transformed epithelia and K19 in simple epithelia (Moll et al. 2008).

Within the keratin family, the type II keratin K80 is unique, in that it is ubiquitously expressed in virtually all types of epithelia and cultured cells thereof (Langbein et al. 2010a; Langbein and Schweizer 2013). Other keratins distinguish themselves by an extremely narrow expression profile such as hair keratins K32 and K82 of the hair cuticle, K84 of the filiform tongue papilla (Langbein and Schweizer 2005), K37 of the medulla of sexual hairs (Jave-Suarez et al. 2004; Langbein and Schweizer 2013; Langbein et al. 2010b), the hair follicle-specific epithelial keratins K26, K72 and K73 of the inner root sheath (IRS) cuticle, K74 of the IRS Huxley layer and K75 that is restricted to the companion layer (Langbein and Schweizer 2005, 2013; Winter et al. 1998). Another keratin belonging to this group is the type II keratin K77, which was originally named K1b, due to its close structural similarity to K1 (Langbein et al. 2005; for recent keratin nomenclature, see Schweizer et al. 2006). We have previously shown that, within the plethora of normal adult human epithelia, both K77 transcripts and proteins are present only in luminal cells of eccrine sweat gland ducts and sweat gland tumors, while they are virtually absent from the epidermis and other adnexal epidermal organs (Langbein et al. 2005).

A recent qPCR-based study of embryonic mouse dorsal skin demonstrated the expression of K77 at embryonic (E) day E14.5, which strongly increased by E15.5 and in situ hybridization (ISH) showed K77 mRNA in suprabasal epidermal layers at E16.5 (Bazzi et al. 2007). However, although aware of our study on the apparent restriction of K77 expression to adult human sweat gland ducts, the authors did not further track the fate of murine epidermal K77 during the later fetal and postnatal phases or in the eccrine sweat glands that are known to specifically arise around E17 mouse foot-pad epidermis (Viallet and Dhouailly 1994; Nakamura and Tokura 2009; Kunisada et al. 2009).

We therefore decided to undertake a detailed K77 expression study at the mRNA and protein level of both human and mouse embryonic and adult skin including eccrine sweat gland-containing areas. In addition, the expression of K77 was compared to that of other keratins known to be sequentially expressed in the developing and mature epidermis. Due to the close similarity of K77 to K1 (Langbein et al. 2005), this required a particularly careful characterization of the respective antibodies, whose specificity could further be validated in *Krt1*$^{-/-}$, *Krt10*$^{-/-}$ and *Krt1*$^{-/-}$/*Krt10*$^{-/-}$ knock-out (KO) mice (Reichelt et al. 2001; Roth et al. 2012; Wallace et al. 2012). We show that K77 is constitutively expressed in luminal duct cells of postnatal and adult human and mouse eccrine sweat glands. It is also demonstrable in suprabasal layers of human epidermis during embryonic development but is lost around birth. In contrast, the suprabasal K77 expression in developing mouse epidermis is continued beyond E16.5 and fully maintained in the adult tissue. Thus, our study unravels a difference in keratin expression between human and murine epidermis that has gone unnoticed to date.

Materials and methods

Tissues and cultured cells

We were able to obtain human skin samples of various body sites at various weeks of pregnancy [WP13, WP14 (palm, scalp, back), WP18, WP19 and WP20 (palm), WP21 (palm), WP38 (stillbirth; groin; paraffin-embedded tissue) and newborn gorilla (palm), died shortly after birth]. Human tissues were obtained either during surgery for medical reasons or from cadavers during pathological investigations (National Tissue Collection, University of Heidelberg, Germany) under institutional approval and included adherence to the Declaration of Helsinki (Ethics Committee, Medical Faculty of the University of Heidelberg, vote: S-221-2012 to L.L.). Mouse skin (back, sole) was from wild-type mice, K1$^{-/-}$-, K10$^{-/-}$- as well as K1$^{-/-}$/K10$^{-/-}$ knockout (KO) mice, from adult, embryonic and postnatal mice at days E12.5, E14.5–E18.5, P0, P5 and P10 (Reichelt et al. 2001; Roth et al. 2012; Wallace et al. 2012). Animals were sacrificed in accordance with the UK Animals Scientific Procedures Act, 1986. All procedures were also approved by the Newcastle University animal ethics committee. Immediately after excision, fresh tissues were snap-frozen in isopentane pre-cooled in liquid nitrogen and stored at −70 °C (for details, see Langbein et al. 2004). Cultures of normal human epidermal keratinocytes (NHEK) and immortalized keratinocytes of human line HaCaT (Boukamp et al. 1988) and mouse (Durchdewald et al. 2007; Riehl 2009) were also investigated. Cells were freshly seeded, grown under high-calcium conditions to sub-confluency, confluency with focal onset of stratification and over-confluency (mostly stratified). Furthermore, NHEK were grown as organotypic cultures (OTCs) in combination with human dermal fibroblasts in scaffold-based dermal equivalents for 1, 2, 3, 8 and 12 weeks as previously described in

detail (Stark et al. 2004; Boehnke et al. 2007). Normal mouse epidermal keratinocytes (NMEK) were grown as OTCs essentially following the same protocol with modified medium, which was used as 1:1 mixture of D10 medium and defined keratinocyte SFM (GIBCO 10744–019) supplemented with K-SFM growth supplements (10 ng/ml hEGF, 10^{-10}M cholera toxin).

Antibodies/antisera

K77 antisera (laboratory designation: T5.1 N, T5.2 N) were produced in our laboratory by injection into guinea pigs of synthetic K77 aminoterminal peptides RVYSTSSSAGS GGGS-(*C*) (hK77; Fig. 1c; Supplementary Fig. S1, in red), as well as SAGIINYQRRTTSS-(*C*) (hK1; Fig. 1c; Supplementary Fig. S1, in blue) to which a cysteine residue was added at one end for coupling to keyhole limpet protein (Peptide Specialty Laboratories, Heidelberg, Germany; see also, Langbein et al. 2005). For further antibodies and their dilution for IIF and western blotting, see Supplementary Table S1. All animal experiments were approved by the German Regional Council, Karlsruhe, Germany by license no. G72/12 (to L.L.). All of our laboratory-made new antisera were treated with the respective antigen/peptide to additionally verify specificity by their blocking capacity. Secondary antibodies (IgG or IgG+IgM) used for IIF were: goat anti-guinea pig, goat anti-mouse, coupled to Cy3 (1:500, red fluorescence) or Alexa 488 (1:200, green fluorescence) (all Molecular Probes). For

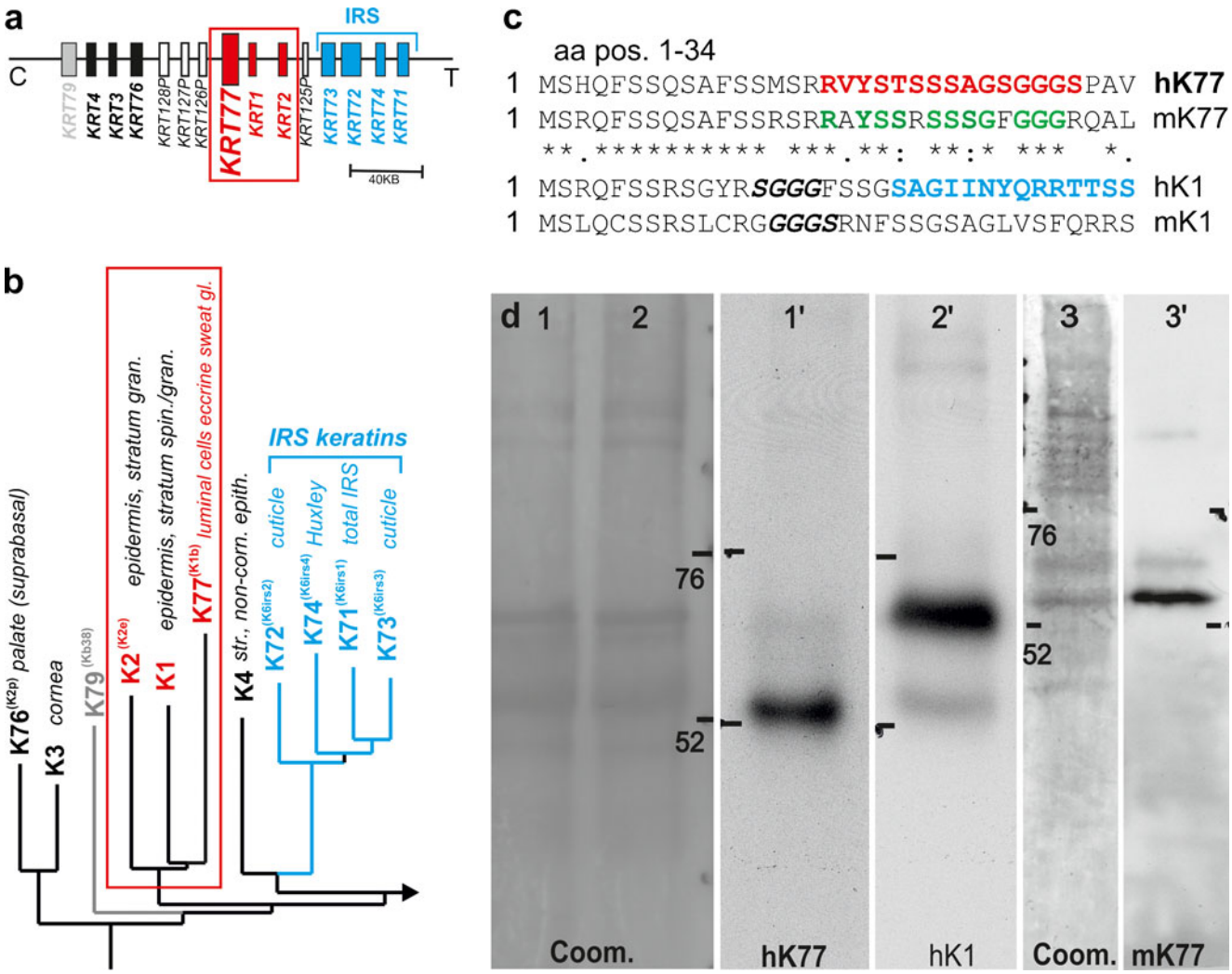

Fig. 1 *KRT77* gene location, phylogenetic position of K77 among keratins, production and specificity of antisera. **a** *KRT77, KRT1* and *KRT2* form a subcluster of differentiation-associated epidermal keratin genes within the partial type II keratin gene locus (*boxed,* in *red*) and **b** the encoded proteins constitute a common branch in a phylogenetic tree (*boxed* in *red*; modified from Rogers et al. 2005). **c** Peptide used for antiserum production of human K77 (hK77, in *red*) and corresponding motif elements of mouse K77 (mK77, in *green*). Sequence homologies in hK77 and mK77 are shown by *. **d** Western blot analysis of hK77 and hK1 antisera. *Lanes 1 and 2* SDS-PAGE of human sole extracts, Coomassie blue-staining. *Lanes 1′ and 2′* hK77 antiserum (T5.2N) and hK1 antiserum (K1.1) detect hK77 at 61.9 KDa and hK1 at 66.0 KDa, respectively. *Lane 3* SDS-PAGE of embryonic mouse back skin, Coomassie blue-staining. *Lane 3′* hK77 antiserum (T5.1N) detects mK77 at 61.4 KDa

chemoluminescence detection (ECL), horseradish peroxidase-coupled rabbit anti-guinea pig IgG (H+L) (Dianova, 1:10,000) were used.

Indirect immunofluorescence (IIF) microscopy

Cryosections were fixed in acetone (−20 °C; 10 min), permeabilized with Tris-buffered saline plus Triton-X100 (TBST:TBS+0.001 % Triton-X100) and blocked with 5 % normal goat serum in PBS. Sections were incubated with primary antibodies for 1 h and, after rinsing in PBS, incubated with secondary antibodies (dilution of 1:200–500) for 30 min. After washing in PBS, sections were dried and mounted. Visualization and documentation were performed with a photomicroscope (Axiophot II equipped with AxioCam digital camera and AxioVision software; Carl Zeiss, Oberkochen, Germany) (for details, see Langbein et al. 2004, 2005). Exclusion of the specific primary antibodies or its replacement with normal serum of untreated animals of the same species or PBS was used as negative controls and also for secondary antibody background evaluation.

Immunoelectron microscopy (IEM)

Ultrathin cryo-sectioning for IEM was performed according to Tokuyasu (Tokuyasu 1989, 1997) with several modifications. Fixation: small pieces of freshly dissected tissue were fixed in 2 % formaldehyde (FA) (in 0.1 M phosphate buffer, pH 7.4; freshly prepared from para-formaldehyde). After the first 15 min of fixation, tissues were cut into ca. 1 mm^3 pieces. After 1 h, the fixative was changed to 1 % FA (in the same buffer) and stored at 4 °C. Preparation for sectioning: fixed tissue pieces were washed 3× for 5 min in PBS. Then, pieces were cooled on a slide on ice and, if needed, trimmed and transferred into 2.3 M sucrose/PBS at 4 °C (overnight). Sectioning: tissue pieces in gelatin were mounted on the specimen holder ("pin") and frozen in the cryo-chamber of the Cryo-ultramicrotome (Leica). The ultrathin sections were mounted on grids. Immuno-labeling with Protein A-Gold: the grids were incubated for melting in 2 % gelatin in a Petri dish (37 °C, 30 min) followed by floating the grids in PBS (37 °C, 20 min). The following steps were done "on drops" on parafilm. Specimens were 2× rinsed with 0,1 % glycine/PBS (2 min, each), incubated with 1 % BSA/PBS (2 min), with the primary antibody in 1 % BSA/PBS/ (1 h), rinsed 4× with 1 % BSA/PBS (2 min, each), incubated with Protein A-Gold in 1 % BSA/PBS (30 min), rinsed 2× with 1 % BSA/PBS (2 min, each) and 4× with PBS (2 min, each). To stabilize the reaction, specimens were incubated on 1 % glutaraldehyde (GA)/ PBS (5 min), 2× washed with PBS (5 min, each), 10× rinsed with freshly distilled water (1 min, each) and 2× rinsed with ice cold methylcellulose (MC)/0.4 % uranylacetate (UA) at room temperature (RT) and incubated on ice-cold MC / 0.4 % UA (5 min). The grids were looped out and the excess of MC/UA was removed with filter paper and then air-dried. For amplification of labeling when the K77 antiserum was used for EM, we modified the above-described method by using 1.4 nm ("nanogold") Fab-fragment-conjugates (1:40 in PBS, 1 h; NanoProbes) as secondary antibody combined with silver enhancement. After rinsing with BSA/PBS (0.05 %, 2×2 min) and PBS (4×2 min) the binding was stabilized by treatment with 1 % glutaraldehyde (5 min) and washed with PBS (2×5 min) and distilled water (10×1 min). Following the instructions of the manufacturer the HQ Silver Enhancement procedure components were freshly prepared before use. Specimens were incubated (ca. 6 min), washed with water (10×1 min), rinsed twice on ice-cold 0.4 % MC/UA, incubated on ice-cold 0.4 % MC/UA (for 10 min) and the excess of MC/UA removed with filter paper. Subsequently, specimens were air-dried. Throughout, for IEM, comparable procedures as for IIF were used as negative controls.

Tissue extraction, gel electrophoresis and western blots

Tissue extracts were prepared from ca. 4–5 skin cryosections (10–15 μm thick) as previously reported (Langbein et al. 2004, 2005). Extracts were resolved by sodium dodecylsulfate-polyacrylamide gel electrophoresis (SDS-PAGE; 10 % polyacrylamide). For western blots, gels were transferred to PVDF membranes (Immobilon-P; Millipore, Eschborn, Germany) by wet blotting. After staining (0.1 % Coomassie blue R250), destaining and blocking with 5 % nonfat milk powder in Tris-buffered saline, membranes were incubated with the respective primary and secondary antibodies (see "Antibodies/antisera"; for all details, see Langbein et al. 2004, 2005).

RNA isolation and quantitative RT-PCR analyses

Total RNA was isolated from skin cryosections using TRIzol® Reagent (Invitrogen) by homogenization (FastPrep FP120 Homogenizer; ThermoSavant). After 5 min incubation (RT), chloroform was added and incubated (3 min, RT). After centrifugation, the supernatant was precipitated and washed with 75 % ethanol. The dried pellet was dissolved in RNase-free water. Total RNA was isolated using RNeasy (Qiagen, Hilden, Germany). One microgram of total RNA was reversely transcribed (ReverseAid™ H Minus First Strand cDNA Synthesis Kit: Thermo Scientific) and qRT-PCR was performed in the LightCycler® 480 II (Roche) with LightCycler® 480 Probes Master mix, forward and reverse primers and UPL-probe (Universal ProbeLibrary; Roche). After preincubation at 95 °C for 10 min, 45 amplification cycles with denaturation (95 °C, 10s) and annealing (60 °C, 30s) were applied. The fluorescence (533 nm) was monitored by LightCycler 480 software 1.5 after each cycle. PCR was stopped by cooling to 40 °C.

For quantification, housekeeping genes (human GAPDH and mouse PGK, respectively) were analyzed in parallel. The ratio of relative mRNA expression of control versus sample was normalized to the housekeeping gene. Verification of the quality of primers/probes combination and the efficiency of the PCR, standard curves were performed for each test. As negative controls, water instead of cDNAs was used. Primers (forward, *f*-; reverse, *r*-) and UPL-sonde (*Nr*-) used: human *hKRT1* (*f*-gcctccttcattgacaaggt, *r*-gctcccattttgtttgcagt; Nr-1), *hKRT77* (*f*-gtgcggacccagtatgaact, *r*-gatctggagctcctggtacttg; Nr-82), *hGAPDH* (*f*-agccacatcgctcagacac, *r*-gcccaatacgacca aatcc; Nr-60), mouse *mKRT1* (*f*-tttgcctccttcatcgaca, *r*-gttttggg tccgggttgt; Nr-62), *mKRT77* (*f*-ggccctgtaccagaccaag, *r*-cttc aggtcgtctccgtgtt; Nr-17) and *mPGK1* (*f*-gaagtcgagaatgcctgtgc, *r*-ccggctcagctttaacctt; Nr-18).

Due to the extremely limited access to human embryonic tissue samples, only technical replicates (n=3) could be made, while for mouse tissues the same number of biological replicates were analyzed.

Results

Sequence characteristics of K77 and specificities of antisera

Within the human type II keratin gene domain on chromosome 12q13, sequentially and functionally related genes such as the IRS keratin genes *KRT71–KRT74*) (Langbein et al. 2003) are subgrouped and form their own evolutionary tree (Fig. 1a, b, in blue). The *KRT77* gene is also subgrouped and forms a tree with the "epidermal differentiation-specific" keratins, K1 and K2 (Fig. 1a, b, boxed in red; for more details, see "Evolutionary history of the *KRT77* gene").

Accordingly, the sequences of human K77 (hK77) and K1 (hK1) are highly similar (Supplementary Fig. S1). Besides highly conserved rod domains, both keratins exhibit conserved non-α-helical H1 subdomains and share distinct glycine-rich sequence stretches in their head and tail domains (Langbein et al. 2005). Because of these similarities, caution had to be taken in the production of a monospecific K77 antiserum to avoid cross-reactivity with K1. In addition, the desired antiserum should also specifically detect the murine ortholog, mK77. For immunization, we therefore selected an oligopeptide of the penultimate hK77 head region (Fig. 1c; Supplementary Fig. S1, in red), which shared 11 out of 15 amino acid positions with mK77 and virtually no epitope with either hK1 or mK1. It should be noted that the same oligopeptide had already been used for immunization in our previous study and successfully been employed for IIF studies (Langbein et al. 2005), while it failed, however, in western blotting. In contrast, when the new K77 antiserum was used for western blotting of total protein extracts of adult human sole skin rich in eccrine sweat glands, it clearly revealed the hK77 keratin band with its calculated molecular weight of 61.8 kDa (Fig. 1d-1′). This antiserum also detected mK77 at 61.4 kDa in extracts of sweat gland-less back skin of mouse embryos (Fig. 1d-3′), thus confirming mRNA data reported previously by Bazzi et al. (2007). Similarly, a specific K1 antiserum produced in our laboratory (Supplementary Fig. S1, corresponding oligopeptide in bold and blue; see also "Materials and methods") detected a strong hK1 band (calc. MW 66.1 kDa) together with an extremely weak band at the position of hK77 (Fig. 1d-2′). This antiserum did not yield bands on blots of mouse skin extracts (not shown).

Expression of K77 in embryonic and adult human skin (IIF)

We investigated human skin samples from various body sites and weeks of pregnancy, i.e., WP13, WP14, WP19, WP20, WP21 and WP38 (stillbirth), as well as from a newborn gorilla, which died shortly after birth. At WP13, the earliest embryonic stage to which we had access, the epidermis consisted of a basal layer, one to two intermediate layer(s) and the periderm (Byrne et al. 2003; Holbrook 2006; Holbrook and Odland 1975) and contained abundant K77 (shown in red) in the intermediate layer(s) (Fig. 2a). Relative to keratins known to be sequentially expressed during epidermal differentiation (shown in green), K77 staining was spatially separated from the K14-positive basal layer of back skin epidermis (Fig. 2b). This pattern was true also for a WP14 scalp section (Fig. 2c). In contrast, double labeling of K77 and K1 in both Fig. 2d (a serial section of Fig. 2c) and Fig. 2e, e′ clearly demonstrated that K1 was expressed earlier than K77 and co-expressed with the latter only in the uppermost intermediate layer. Note that the hair placode (pl) in Fig. 2c (green arrow) and d was negative for K77 and K1 but positive for K14 (Fig. 2c). As shown in Fig. 2f, f′, f″, double-labeling for K77 and K10 mirrored that of K1/K77 in virtually all aspects. K77, K1 and K10 staining up to the uppermost intermediate cell layer was confirmed by double-labeling with a K4 antiserum, which specifically decorated the large cuboidal human periderm cells (shown for K77 and K4 in Fig. 2g).

Interestingly, a closer inspection of the K77/K1 and K77/K10 double-label sections suggested a difference in the intracellular location of K77 relative to that of K1 and K10. This was clearly evident in Fig. 2f′. Whereas K10 was distributed "normally" throughout the entire cytoplasm (Fig. 2f′, green arrows), K77 seemed to be more concentrated around the nucleus (Fig. 2f′, red arrows; see also next section).

The chronological order of keratin expression was also investigated at the respective embryonic stages in the distinctly thicker palmar epidermis. In this anatomical region, K14 expression at WP14 was not restricted to the basal layer proper but extended into the para- and lower suprabasal compartments, whereas K77 was detectable in the upper strata with only few K77/K14-co-expressing cells (Fig. 2h; serial sections

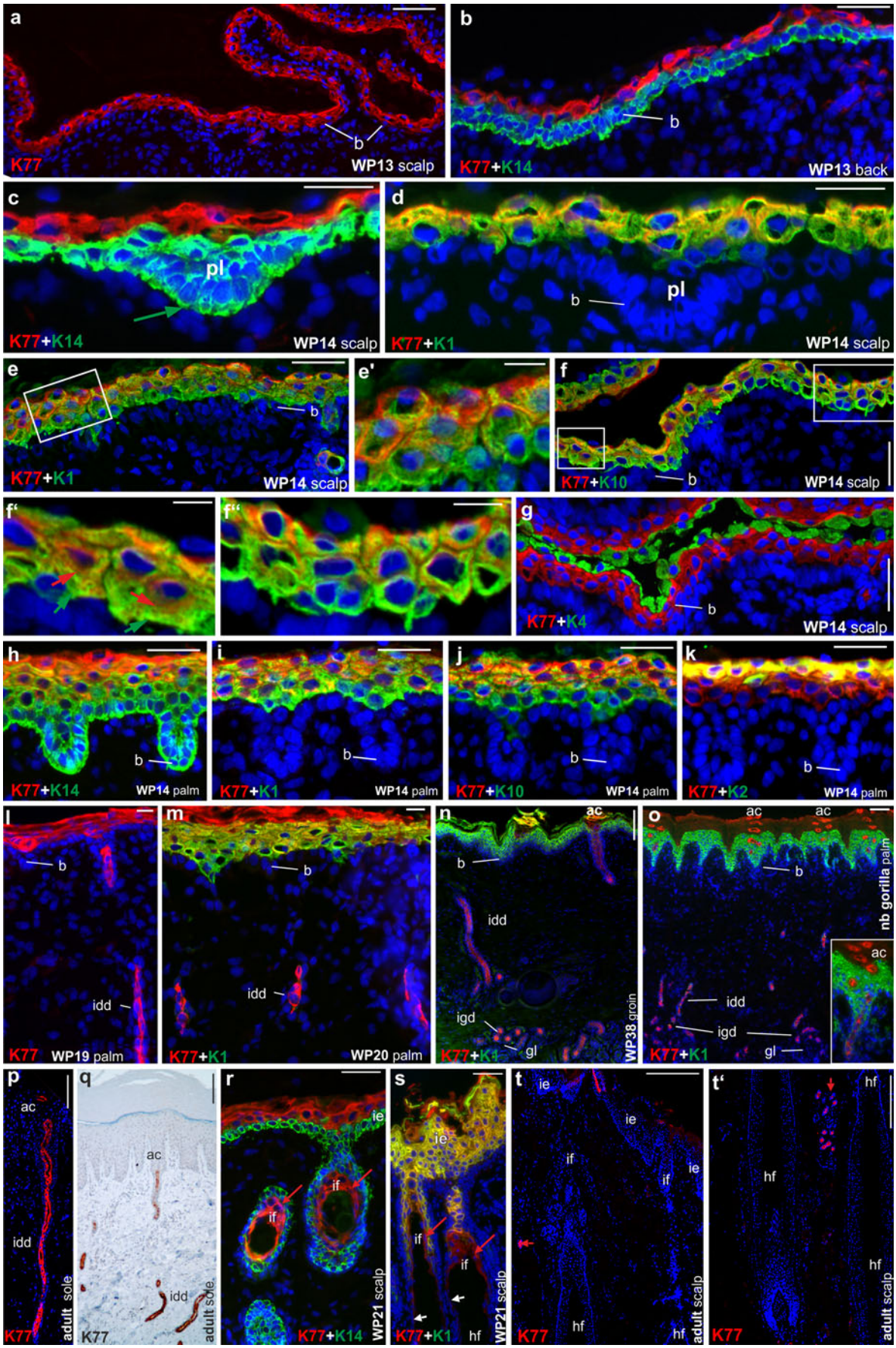
a
b
K77
WP13 scalp
K77+K14
WP13 back
c
d
pl
K77+K14
WP14 scalp
K77+K1
WP14 scalp
e
e'
f
K77+K1
WP14 scalp
K77+K10
WP14 scalp
f'
f''
g
K77+K4
WP14 scalp
h
i
j
k
K77+K14
WP14 palm
K77+K1
WP14 palm
K77+K10
WP14 palm
K77+K2
WP14 palm
l
m
n
o
idd
K77
WP19 palm
K77+K1
WP20 palm
ac
igd
gl
WP38 groin
nb gorilla palm
p
q
r
s
t
t'
adult sole
K77
K77+K14
WP21 scalp
K77+K1
hf
adult scalp
ie
if

◀ **Fig. 2** Expression of K77 in embryonic and adult human skin (IIF). K77 (in *red* throughout) in parabasal layer of scalp (a, c) and back skin (b). The basal layer is negative for K77 (a, b, c) but positive for K14 (b, c, *green*). Placodes are K77 and K1 negative (c, d). K77 (d–f″, *red*) is expressed slightly later than K1 (d–e′; *green*) or K10 (f–f″, *green*). Note that K77 filaments (f′–f″, *red arrows* in f′*)* but not K10 filaments (f′–f″, *green arrows* in f′) seem to be concentrated around the nucleus. Periderm cells are K4 positive (g, *green*) but K77 negative (g, *red staining of intermediate layer*). Higher stratified palm skin shows sequential expression of K14, K1, K10 (*green*) and K77 (h–j). K2 is the last keratin expressed (k, *green*). Incipient rete ridges are negative for K77, K1, K10 and K2 (i–k). At WP19 and WP20 (l, m), K77 (*red*) is present in the epidermis and sweat gland ducts, where K1 is missing (m; *green*). Around birth, K77 (*red*) is restricted to the sweat gland intraglandular and intradermal ducts (n–o, *igd, idd,*) and the acrosyringium (*ac*) but lost in the epidermis of man (n) and newborn gorilla (o, *nb gor*), which are both positive for K1 (n, o, *green*). Secretory sweat glands (*gl*) are K77-negative (n, o). The same holds true for adult human skin (p, *by IIF*; q, by *immunoperoxidase*). In embryonic skin, K77 (in *red*) is present in interfollicular epidermis (*ie*) and the infundibulum (*if*) of hair follicles (r, s). In adult skin, K77 is only present in the eccrine sweat gland duct and acrosyringium, respectively (t, t′). *WP* week of pregnancy; *b* basal layer; *pl* placode; *idd* intradermal-; *igd* intraglandular eccrine sweat gland duct. *Bars* (a–f, g–m, r, s) 10 μm; (e′, f′, f″) 5 μm; (n–q, t, t′) 200 μm

in h–k). K77/K1 and K77/K10 double-labeling confirmed that both K1 (Fig. 2i) and K10 (Fig. 2j) expression clearly preceded that of K77, while K2 and K77 were co-expressed only in the uppermost epidermal layer (Fig. 2k, merged yellow). At both WP19 and WP20, K77 was still present in the upper epidermal cell layers (Fig. 2l, m), where its expression was preceded by that of K1 (Fig. 2m) but also clearly visible in the developing eccrine sweat gland intradermal ducts (Fig. 2l, m, idd).

As we had no access to embryonic skin samples beyond WP20, the investigation of K77 expression during human embryonic development could only be resumed in groin skin of a WP38 stillbirth. We show that at this quasi full-term stage, for the first time K77 was no longer demonstrable in the suprabasal K1-positive human epidermis (Fig. 2n, in green) but clearly present in the acrosyringium (ac) and the intradermal (idd) and intraglandular (igd) duct of now functional eccrine sweat glands (Groscurth 2002; Holbrook 2006) (Fig. 2n, in red). It is worth mentioning that exactly the same observations held true for palmar skin of a newborn gorilla (Fig. 2o). The strict limitation of K77 expression to the eccrine sweat gland intradermal ducts (idd) and acrosyringia (ac) in the glabrous sole of adult humans is shown in Fig. 2p (by IIF) and q (by immunoperoxidase).

As Fig. 2c, d had shown that K77 and K1 are absent from very early embryonic stages of hair follicle formation, we investigated its fate in later stages. Besides K77 expression in the suprabasal interfollicular epidermis (ie) of embryonic scalp skin, we also detected the keratin in the infundibulum (if) of hair follicles of WP21 embryos (Fig. 2r, red arrows), where it was largely co-expressed with K1 down to the transition into the isthmus (Fig. 2s, merged yellow). In contrast, K77 was absent from any compartment of the adult hair follicle (Fig. 2t, t′, hf).

Expression of K77 in adherent and organotypic cultures (OTC) of human keratinocytes

We used the immortalized human keratinocyte line HaCaT in order to test whether K77 is expressed in epidermal cell cultures. As shown in Fig. 3a, 2 days (d) old HaCaT monolayer cultures indeed exhibited few individual K77-positive cells. After 5d, HaCaT cells stratified locally, building up multilayered cell "domes", only the suprabasal cells located at the apex, were K77-positive (Fig. 3b). This pattern progressed with time leading to larger K77-positive cell areas (Fig. 3c, d, 8d and 12d, respectively). Double-label studies of K77 with K1 showed K1-positive cell assemblies, with the central suprabasal cells co-expressing K1 and K77 indicating that in vitro K1 is also expressed earlier than K77 (Fig. 3e, 5d and 3f, 12d). Investigations of NHEK (not shown) grown both subconfluently and "over"-confluently (with cell "domes") showed similar results with K77 being present in the suprabasal cells. In contrast to the situation in adult epidermis, however, in both keratinocyte types even the uppermost cells obviously do not reach the "adult skin" differentiation state and do not switch off K77 expression.

Akin to embryonic epidermis, K77 preferentially adopted a perinuclear location (Fig. 3f; f′, g, red arrows) so that the remaining peripheral cytoplasmic region was only stained for K1 (Fig. 3f′, g, green arrows). Double-labeling for K77 and desmoplakin (dp) revealed that the K77-containing IF-network did not seem to abut onto the dp-staining along the punctate desmosomes but seemed to leave an unstained interspace region (Fig. 3h, white arrow), which was, however, only focally visible by IIF at light microscopic level. In contrast, staining the cultures for K1 showed the classical intracellular pattern with the K1-containing filaments completely traversing the cytoplasm and anchoring at the desmosomes at the inner aspect of the cell membrane (Fig. 3i, red and green arrows). Finally, and again like in vivo (Fig. 2k), K2 (green) was co-expressed with K77 (red) as the last keratin in the uppermost cells (Fig. 3j, 13d).

In addition to adherent keratinocyte cultures, K77 expression was investigated in organotypic cultures of normal human keratinocytes. Figure 3k revealed that 7-day-old OTCs were positive for K1 but negative for K77 in suprabasal cells. In these, an increasingly positive K77 reaction was, however, seen in 14-day-old cultures (Fig. 3l). At this time, K14 expression extended substantially above the basal layer thus merging with K77 in the upper layers (Fig. 3l′). Double-label staining of K77 with K1 confirmed the earlier onset of K1 expression in the suprabasal compartment (Fig. 3m). With increasing time, the K1/K77 expression patterns approached more towards that of the late embryonic sole epidermis

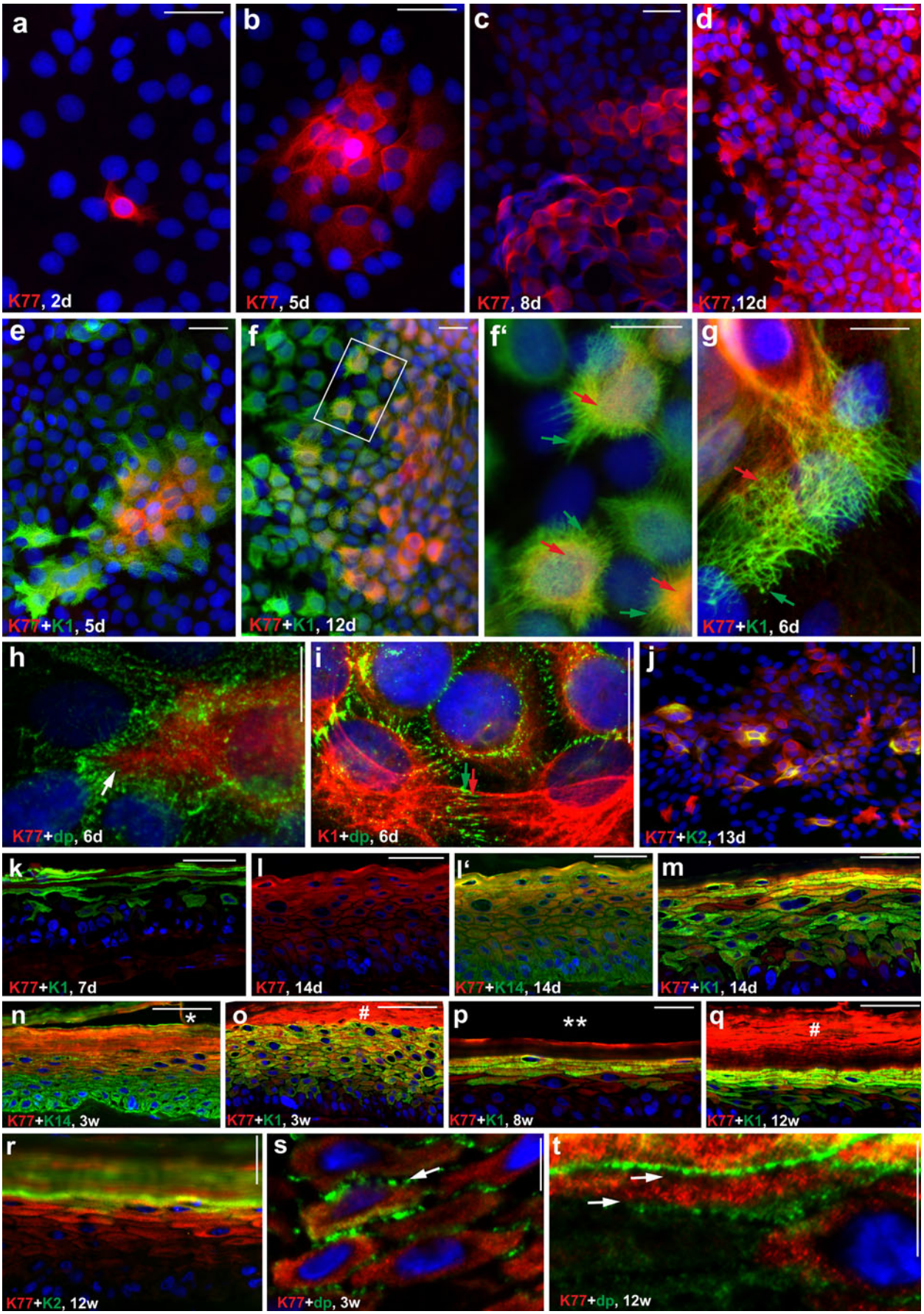
a
K77, 2d
b
K77, 5d
c
K77, 8d
d
K77,12d
e
K77+K1, 5d
f
K77+K1, 12d
f'
g
K77+K1, 6d
h
K77+dp, 6d
i
K1+dp, 6d
j
K77+K2, 13d
k
K77+K1, 7d
l
K77, 14d
l'
K77+K14, 14d
m
K77+K1, 14d
n
*
K77+K14, 3w
o
#
K77+K1, 3w
p
**
K77+K1, 8w
q
#
K77+K1, 12w
r
K77+K2, 12w
s
K77+dp, 3w
t
K77+dp, 12w

◀ **Fig. 3** Expression of K77 in adherent and organotypic cultures (OTC) of human keratinocytes. In adherent HaCaT cultures (a–j) K77 expression starts in single cells (a, in *red*). Increasing cell density leads to a steadily increasing accumulation of K77-positive cells (b–d) that are surrounded by K1-positive cells (e–f, *green*), indicating that K1 is expressed before K77. Unlike K1 filaments (f, g; *green arrows*), K77 filaments do not reach the cell membrane (f′–g, *red arrows*). Double-label staining in the keratinocytes reveals an unstained area (h, *white arrow*) between K77 filaments (h, *red*) and desmoplakin (h, *dp*, in *green*) that is not seen by double-label staining for K1 (i, *red arrow*) and desmoplakin (i, *green arrow*). Single, uppermost HaCaT cells co-express K2 (*green*) and K77 (*red*) (j, *merged yellow*). Normal human keratinocytes grown as OTCs start K1 expression (k, in *green*) before K77 (k, *negative*), which, however, occurred suprabasally by 14d of cultivation (l, l′, *red*). At this time, K14 was present in most cells (l′, *green*), while K1 expression (m, *green*) preceded that of K77 in suprabasal cells (m, *red*). This pattern was essentially retained after 3w (n, o), 8w (p) and 12w (q) of cultivation. In the latter, K2 is expressed in uppermost cells (r, *green*). Again, a K77-unstained rim at the cell membrane is seen by *dp* double staining (s, t, *green, white arrows*). Note that, unlike fully developed epidermis in vivo, K77 did not disappear from OTCs. *d* days of growth; *w* weeks of cultivation. *Bars* (a–f, j–r) 20 μm; (f′, g–I, s–t) 10 μm

(compare Figs. 2h and 3n for K14/K77 as well as Figs. 2i and 3o for K1/K77). K77 labeling was increasingly restricted to the stratum corneum while K14 and K1 were seen in the underlying layers with only marginal co-expression in the increasingly compact epithelium (Fig. 3n; o, #) from which the stratum corneum was often shed or lost (Fig. 3n, *, p, **). Similar to the epidermis in vivo, K2 is only seen in the uppermost suprabasal layer(s) (Fig. 3r, merged yellow) and double labeling of K77 and desmoplakin (dp) confirmed the centrally concentrated intracellular staining of K77 (Fig. 3s, t, white arrows).

Subcellular localization of K77 and K1 in human and mouse skin by immunoelectron microscopy (IEM)

To further study the unique intracellular location of K77 IFs described above, the distribution of gold-labeled K1 and K77 was investigated by immunoelectron microscopy (IEM) in human WP21 skin samples. While basal cells were negative for K1 (Fig. 4b-c, bc), in spinous cells K1-filaments were strongly labeled and entered the desmosomes (Fig. 4a-c, ssc, arrowheads). As the K77 antiserum was markedly less sensitive in IEM than that of K1, we utilized 1.4 nm ("nanogold") - labeled Fab-fragments in combination with silver-enhancement of the labeling instead of using the complete 10 nm-labeled secondary antibody (see "Materials and methods"). As shown in Fig. 4d, this approach considerably increased the staining intensity of K77 in spinous cells exhibiting a prominent labeling of cytoplasmic keratin filaments and an unlabeled zone between the cell membrane and the cytoplasmic K77-positive IF network (Fig. 4d and insert, triangles, broken lines).

This particular IF pattern was previously demonstrated in the duct of eccrine sweat glands in which K77 is restricted to luminal cells and co-expressed with a large number of other keratins (K6, K5, K10, K14, K16, K17, K19) (Langbein et al. 2005). The resulting extremely dense IF network accumulating asymmetrically in the cell area facing the lumen (Supplementary Fig. S2c–g′) has previously been taken for a "cuticle" (Heynold 1874; Stöhr 1906) (Supplementary Fig. S2a, b). This specific IF network emerges around the 6th month of gestation (Hashimoto et al. 1966) and, together with the numerous desmosomes (Supplementary Fig. S2g-g′), forms a compact periluminal keratin belt along the entire duct. Despite these densely packed IFs, immunogold labeling (Supplementary Fig. S2c, d; at light microscopy) and IEM enabled us to demonstrate that K77 IFs again keep distance from the desmosomes (Supplementary Fig. S2h, broken lines).

Expression of K77 in mouse embryonic and adult skin (IIF) including adherent and organotypic keratinocyte cultures

Since our collection of human embryonic skin samples did not allow us to determine the whole interval of fetal K77 expression, i.e., stages before WP13 (timepoint of K77 expression onset) and subsequent to WP21 up to birth (timepoint of epidermal K77 expression end), we decided to investigate the fate of K77, together with that of K1 and K10, during the murine gestation period. In accordance with Bazzi et al. (2007), neither K77 (Fig. 5a) nor K1 and K10 (not shown) could be demonstrated in E12.5 epidermis, while by E14.5 both K77 (Fig. 5b, K77 in red, K14 in green) and K10 expression (Fig. 5c, K77 in red, K10 in green, merged yellow) but not K1 expression (Fig. 5d) was detectable in the upper intermediate layers. This changed at E16.5 at which K77 and K10 expression became equally strong in suprabasal (including parabasal) cells (Fig. 5e, f), while the onset of K1 expression seemed to occur slightly later (Fig. 5g; cf. also j). As expected, all three keratins were absent from the extremely flat, K4-positive mouse periderm cells (Fig. 5h). K77 double-label studies revealed that these patterns were essentially maintained up to birth. K77 expression started in parabasal cells with only partial K14 co-expression (Fig. 5i). In contrast to humans, murine K1 expression was clearly delayed compared to that of K77 by at least one cell layer (Fig. 5j), while the latter continued to completely overlap with K10 from parabasal cells upwards (Fig. 5k).

Surprisingly, unlike the expression pattern of human K77, murine K77 expression was maintained in the epidermis after birth (Fig. 5l–n). Oblique (Fig. 5l) and horizontal cross-sections (Fig. 5m, n) through the distal pads of the fore-foot of a 10-day-old mouse showed strong expression of K77 (Fig. 5l, m) and co-expression with K10 (Fig. 5n), in the suprabasal epidermis as well as in the suprabasal layer of eccrine sweat gland ducts (Fig. 5l, m, sgd).

In line with human hairy skin, K77 was completely absent from early embryonic hair follicles (hf) (Fig. 5o,

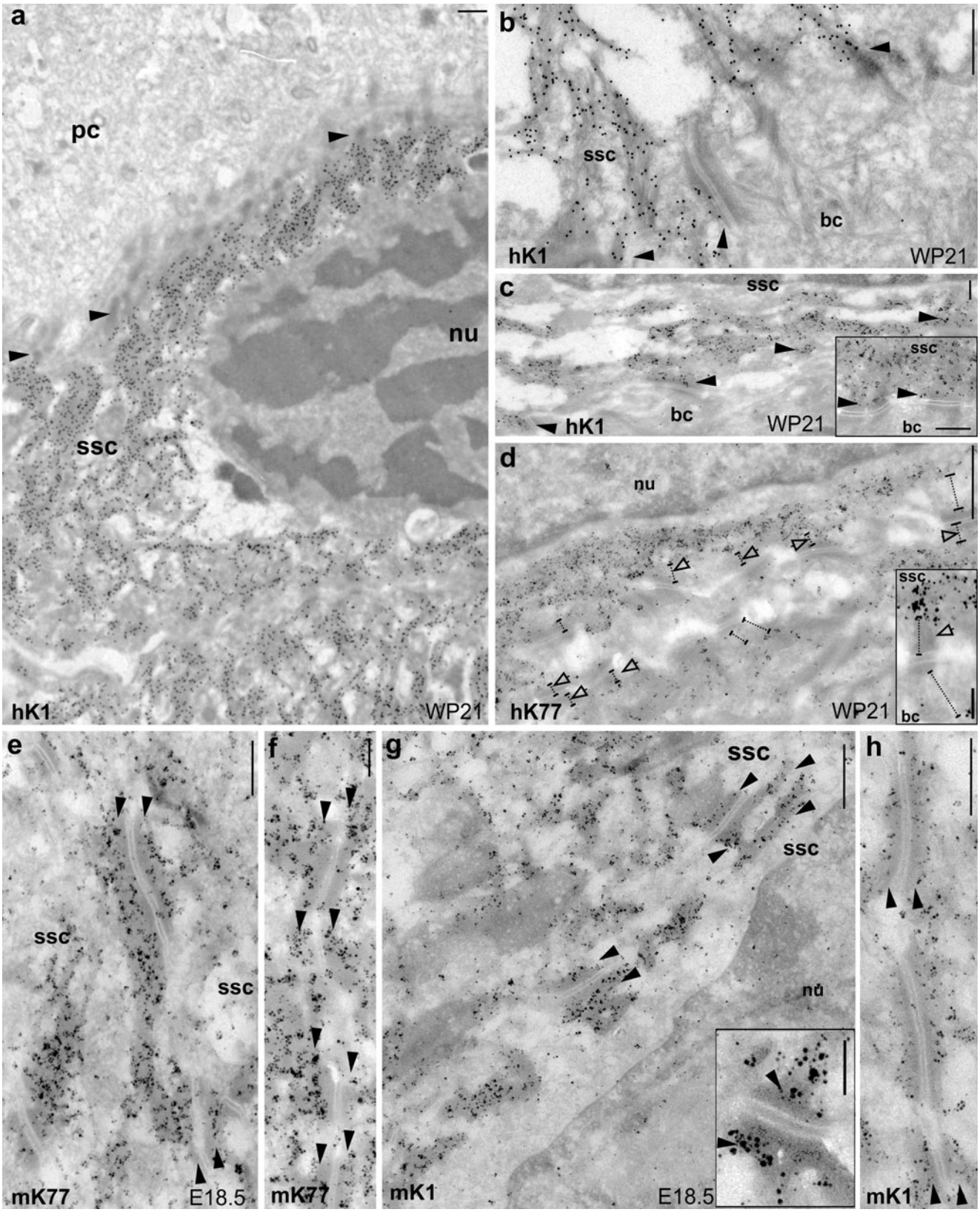

E16.5; Fig. 5p, q, E18.5) as well as fully developed follicles of adult back skin (Fig. 5r-r′, hf). Independent of the different developmental stages, K77 was present throughout the interfollicular epidermis (Fig. 5p, q, ie)

◀ **Fig. 4** Immunoelectron microscopic localization of K77 and K1 in human and mouse skin by immunogold staining. In human embryonic epidermis at week of pregnancy (*WP*) 21 (a–d, *WP21*) a strong cytoplasmic labeling of hK1 filaments attached to desmosomes is seen in *str. spinosum* cells (*ssc*) but not in basal (*bc*) and periderm- (*pc*) cells (a–c, *arrowheads*). In contrast, an hK77-unlabeled area is seen at cell membrane near desmosomes (d, *dotted lines, triangles*). In embryonic mouse epidermis (e-h, *E18.5*), both labeled cytoplasmic mK77 (e–f, *arrowheads*) and mK1 filaments (g–h, *arrowheads*) insert into the desmosomes. 15 nm gold (a, b) and 1.4 nm gold on Fab-fragments label with silver enhancement (c–h) of *ssc* cells. *Bars* (a, b, d, e, g) 500 nm; (c, f) 250 nm; (h, inserts in c, d, e) 125 nm

and the embryonic (Fig. 5p, insert) and adult follicular infundibulum (Fig. 5r, r′, if).

The expression of K77 in immortalized mouse keratinocytes followed the same trend as in human keratinocytes (see Fig. 3k–r). Initially, randomly scattered K77-positive cells increased in number with time, cell density and the number of differentiating cell heaps within the cultures (Supplementary Fig. S3a, b). Similarly OTCs of normal murine keratinocytes expressed K77 from parabasal cells upwards (Supplementary Fig. S3c). Double label studies with K14 highlighted the abrupt beginning of strong K77 expression in parabasal cells (Supplementary Fig. S3c′), which was more diffuse in the corresponding human OTCs (Fig. 3l′), as well as K77/K14 co-expression in the lower spinous cells (Suppl. Fig. S3c′). Again as observed in embryonic and postnatal mouse epidermis (Fig. 5g, j), K77 was noticeably expressed earlier than K1 (Supplementary Fig. S5d). Finally, in both human and murine keratinocyte OTCs, K77 strongly accumulated in the stratum corneum (compare Fig. 3n–r and Supplementary Fig. S3c, d).

More importantly, immunogold IEM labeling revealed another difference between the intracellular localization of human and murine K77 in that IFs of the latter displayed the conventional distribution throughout the total cytoplasm including the attachment to the desmosomal plaques (Fig. 4e, f, arrowheads) thus behaving like K1 IFs (Fig. 4g and insert, h; arrowheads).

K77 and K1 mRNA expression during mouse and human skin development

We undertook RT-PCR studies in order to investigate the complex course of keratin gene expression in embryonic and postnatal mouse and human skin of different anatomical localizations at the mRNA level. K77 and, at a somewhat lower level, K1 mRNA were expressed by E15.5 (Fig. 6a; see also Bazzi et al. 2007). Up to birth, K77 mRNA values dropped while K1 values increased and this trend was reversed after birth, when K77 mRNA expression peaked at P10 (Fig. 6a). In line with the corresponding protein data, the latter consisted mainly in epidermal K77 mRNAs but a considerable fraction of K77-transcripts likely originated from the luminal duct cells of the large number of functional eccrine sweat glands (cf. Fig. 5l, m) (Byrne et al. 2003; Cui et al. 2012; Taylor et al. 2012) in the protruding pads of sole skin. The same K77/K1 mRNA trend was observed in age-matched postnatal back skin (Fig. 6a, dashed columns), which was, however, completely free of eccrine sweat glands. In this case, the value of K77 transcripts determined in back epidermis probably included transcripts expressed in the infundibulum of the countless hair follicles present in back skin (cf. Fig. 5r, r′).

In human skin, the K77 mRNA values differed only marginally between embryonic and adult skin samples, a finding that could be correlated with the corresponding protein data. While WP14 sole skin contained few suprabasal K77-positive epidermal cell layers (Fig. 6b, left column; cf. Fig. 2i), the keratin was completely absent from mature epidermis (cf. Fig. 2n, o) but instead present in luminal duct cells of eccrine sweat glands (cf. Fig. 2n, o and Fig. 6b, middle column). Apparently the total mass of K77-positive luminal cells of the intradermal and -glandular ducts of sweat glands slightly exceeded that of K77-expressing epidermal cells in WP14 sole. Although eccrine sweat glands contributed to the K77 mRNA value of adult scalp skin, their smaller density is in line with the lower amount of K77 transcript at this body site (Fig. 6b, right column). Conversely, the considerably higher increase in K1 mRNAs observed in adult versus WP14 embryonic sole and scalp skin (Fig. 6c) was caused by the much higher number of K1-positive cell layers in adult sole (Fig. 6b, middle column) and, to a lesser extent, scalp skin (Fig. 6b, right column). The mRNA data and the corresponding protein data were obtained from three technical replicates of the same human tissue sample, used either for RNA isolation and qPCR or for IIF.

In human keratinocytes grown as OTCs, the extent of K77 and K1 mRNA expression over time in culture (Supplementary Fig. S4, red and green columns, respectively) correlated with the increasing number of cell layers positive for K77 or K1 protein (see, Fig. 3k, 7d; m, 14d; o, 21d) and was comparable to the data obtained from tissues in vivo.

It should be mentioned that the K77 expression scenario depicted here exemplifies the risks of interpreting expression studies solely based on mRNA data frequently derived from micro-array analysis. Attempts to judge the K77 expression characteristics in the developing human skin by PCR-based RNA data alone would be misleading since the developmental switch of K77 expression from epidermis to sweat glands would go unnoticed.

Expression of K77 in *Krt1*$^{-/-}$-, *Krt10*$^{-/-}$- and *Krt10*$^{-/-}$+ *Krt1*$^{-/-}$ mice during embryonic skin development

To gain additional insight into the expression characteristics of K77 and K1 as well as their putative type I partners K14 and K10, we investigated the fate of these keratins during skin development in *Krt1*$^{-/-}$- and *Krt10*$^{-/-}$-KO as

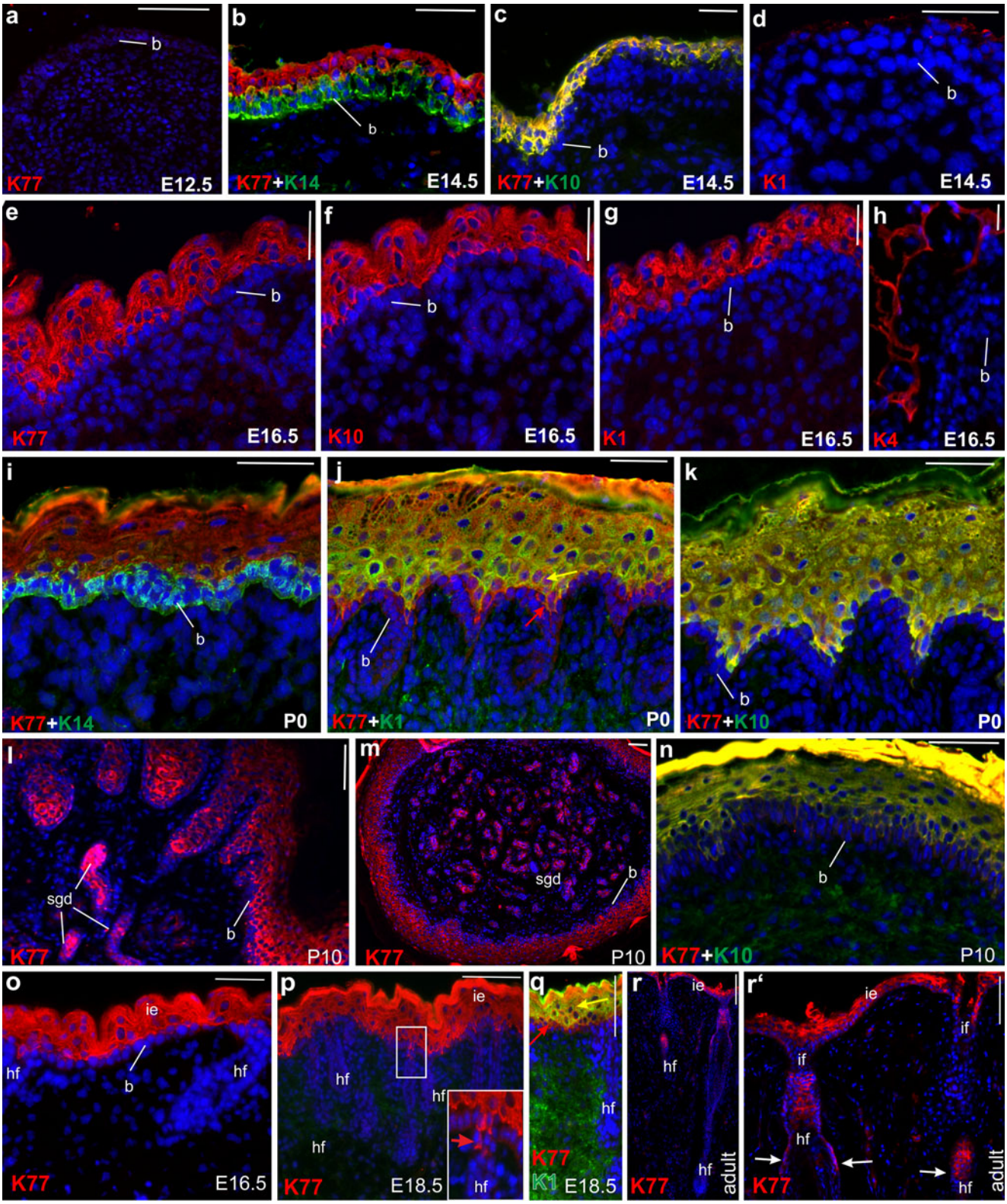

well as $Krt10^{-/-}+Krt1^{-/-}$ -double KO mice (Reichelt et al. 2001; Roth et al. 2012; Wallace et al. 2012). As mice from K1- and K1+K10-deficient lines die at the day of birth due to severe lesions caused by suprabasal epidermal fragility (Roth et al. 2012; Wallace et al. 2012), the investigated time frame was set from E17.5, when K77 is already expressed, to P0. By

◀ **Fig. 5** Expression of K77 in embryonic and adult mouse skin (IIF). By embryonic day E12.5 mouse skin is K77 negative (a). By E14.5 keratin K14 (b, *green*) is seen in basal cells and K77 (b, c, *red*) and K10 (c, *green/ yellow merged*) in suprabasal cells that are still negative for K1 (d). At E16.5 K77 (e), K10 (f) and K1 (g) are abundantly expressed in suprabasal cells. The extremely flat mouse periderm cells are K4-positive (h). At birth, K14 is restricted to basal cells (i, *green, b*) whereas K77 is present in suprabasal cells (i; *red*). Note that in the mouse, K77 (j and q, *red; red arrows*) is expressed earlier than K1 (j and q, *green/ yellow merged*) but shows clear co-expression with K10 (k and n, *green/ yellow merged*). After birth K77 is present in epidermis and in fully developed eccrine sweat gland ducts in the foot pads (l–m, *sgd*). Whereas mouse interfollicular skin (o–r′, *ie*), including the infundibulum (o–r′, *if*), is K77-positive, hair follicles (o–r′, *hf*) are left unstained in both embryonic (o–q) and adult (r–r′) back skin. *b* basal cell layer. *Bars* (a–d) 10 μm; (e–k, o, p) 20 μm; (l–n, q–r′) 50 μm

E17.5, at which sole epidermis of $K1^{-/-}$ mice is already highly stratified, suprabasal K77 expression started in parabasal cells, which exhibited a weak co-expression with the basal keratin K14 (Fig. 7a, a′ and insert), while K77 and K10 showed a complete suprabasal co-expression (Fig. 7b, b′). Although severe damage, i.e., ruptures and vacuolization occurred in suprabasal epidermal cell layers of P0 sole skin (Fig. 7c, d,*), double-label studies with both K77/K14 and K77/K10 combinations yielded epidermal expression patterns not only similar to those seen in E17.5 skin of $K1^{-/-}$ mice (cf. Fig. 7c, d and a, b) but also to those of age-matched normal mice (cf. Fig. 5i, k). Surprisingly, despite a noticeable more injured epidermis, the same observations held true also for $K10^{-/-}$+$K1^{-/-}$ mice, where, in addition to the sequential K14/K77 pattern (Fig. 7e), the staggered suprabasal K77/K2 pattern also seemed to remain largely undisturbed (cf. Fig. 7f, f′; cf. Fig. 2k). Together, these studies revealed that not only the loss of K1 but also that of K1+K10 did not visibly influence the normal sequential expression path of K14 and K77.

Moreover, studies in *Krt10*$^{-/-}$ mice showed that, in the absence of this keratin, K77 was co-expressed with K14, which in addition to the basal layer was also expressed in the suprabasal epidermis from E14.5 embryos up to adult animals (Supplementary Fig. S5a, c, e, h; see also Fig. 3l′ and Reichelt et al. 2004).

In addition and more importantly from a technical point of view, the studies in KO mice tissues unambiguously proved the mono-specificity of the K77 and K1 antibodies raised in our laboratory.

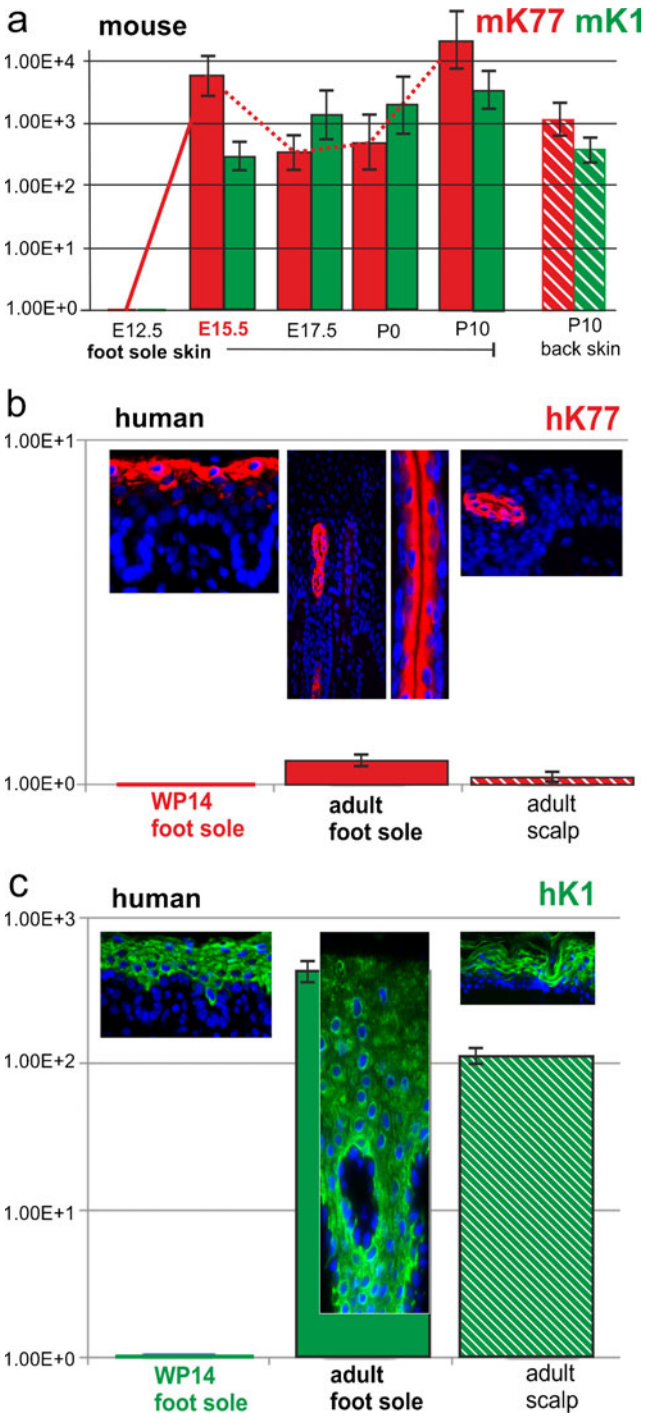

Fig. 6 PCR monitoring of K77 and K1 mRNA during human and mouse ▶ skin development. **a** Mouse K77 mRNA expression level at E12.5 was defined as 1 (*arbitrary unit*). By E15.5 K77 mRNA (*red*) and K1 mRNA (*green*) are strongly but variably enhanced until birth in both sole skin (*solid bars*) and back skin (*striated bars*). *Error bars* show the standard deviation of biological replicates (n=3). **b** In human sole skin at WP14, hK77 mRNA (*red column*) is weakly (1 *arbitrary unit*) expressed as is hK77 protein in a few suprabasal epidermal layers. In contrast, hK77 mRNA is moderately enhanced in adult sole skin (*red column*) with hK77 protein being, however, present only in the numerous sweat gland ducts. To a lesser extent, these patterns also hold true for adult scalp skin (*striated column*), containing fewer sweat glands. **c** Corresponding analysis of hK1 mRNA and protein (in *green*), yielding higher values than hK77 at both skin sites. Note that the samples used for normalization represent different states in murine and human skin embryonic development. The mRNA isolation and protein labeling by IIF were done from serial sections of the respective human tissues. *Error bars* show the standard deviation of technical replicates (n=3)

Evolutionary history of the *KRT77* gene

To gain insight into the evolutionary origin of the *KRT77* gene as well as its possible phylogenetic relationship to the *KRT1* and *KRT2* genes, we screened a broad range of publicly available genome sequences of vertebrates for orthologs of *KRT77*. Putative *KRT77* orthologs were detected in mammals but not in sauropsids and anamniotes. To ascertain this result, which was in agreement with a recent study of Vandebergh and Bossuyt (2012), we scrutinized a chromosomal sequence contig containing the *KRT77*/*KRT1*/*KRT2* cluster in the most basal extant mammal, that is, the platypus (*Ornithorhynchus anatinus*) (Supplementary Fig. S6). Although numerous gaps in the draft genome sequence of this species precluded the full determination of the gene structures, an ortholog of *KRT77* could be unambiguously identified (Fig. 8a). As in the human genome, putative *KRT1* and *KRT2* genes were located adjacent to the *KRT77* gene of the platypus. Interestingly, a gene with an apparently functional exon–intron structure and an intact open reading frame was detected at a position corresponding to that of the human pseudogene *KRT125P* (Fig. 8a). When the partial amino acid sequence prediction for platypus K77 was compared to other keratins, a highly conserved and K77-specific sequence motif at the C-terminus was detected (Fig. 8b). By contrast, the putative K2 homolog of the platypus showed poor conservation of the C-terminus while the C-terminus of platypus K1 remained elusive. Because the currently available platypus genome sequence is incomplete, the N-terminal sequence could only be determined for K1 and K2 but not for K77 (Supplementary

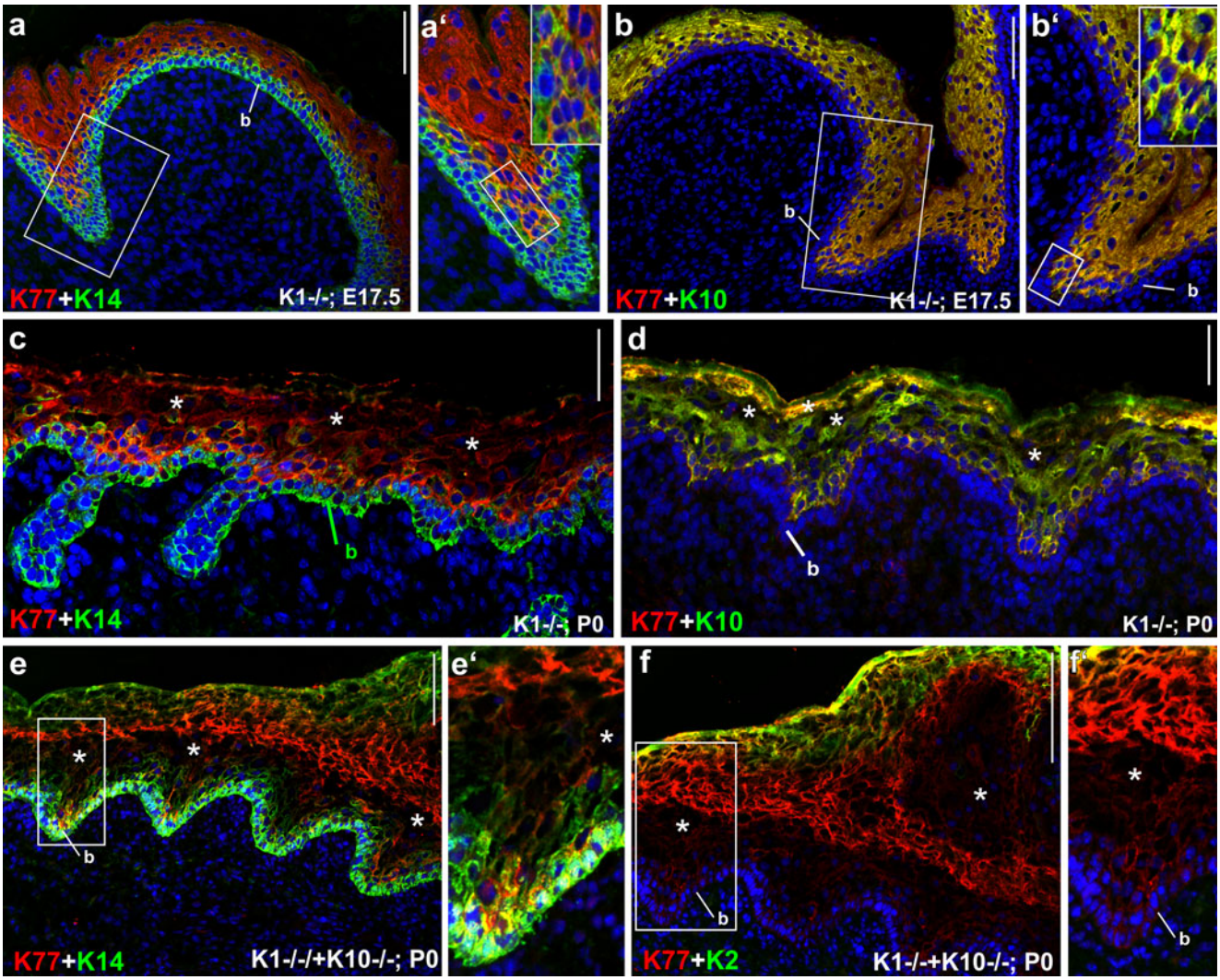

Fig. 7 Expression of K77 in *Krt1*$^{-/-}$ and *Krt10*$^{-/-}$ + *Krt1*$^{-/-}$ mice during embryonic skin development. By E17.5, embryonic foot pad skin of K1$^{-/-}$ KO-mice (a–b′) shows normal K14 expression in basal cells (a, a′, *green, b*) and K77 in suprabasal layers (a, b, *red*) as well as suprabasal co-expression of K77 (*red*) and K10 (b, b′, *red/ merged yellow*). Ruptures (*) in the suprabasal epidermal compartment are, however, seen at birth in K1$^{-/-}$- (c, d, *P0*) and K1$^{-/-}$+K10$^{-/-}$ mice (e–f′, *P0*). Note that, in the latter, K10 is partially replaced by K14 in lower suprabasal layers below ruptures (e′, *green/merged yellow* with K77). K2 remains in the uppermost epidermal layers (f, f′, *green/ merged yellow*). *b* basal cell layer. *Bars* (a–b, e–f) 100 μm; (c, d) 50 μm

Fig. S7). Taken together, our investigation by comparative genomics suggested that K77 originated after the divergence of mammals and sauropsids (Fig. 8c) and that unique features such as its carboxy-terminal sequence were already present in early mammals. Thus, K77 is an ancient and presumably important component of the mammalian integument.

Discussion

In this study, we have extended previous investigations on the expression characteristics of the type II keratin K77 in man and mouse (Bazzi et al. 2007; Langbein et al. 2005). We show that apparently inconsistent findings, which suggested its exclusive expression either in eccrine sweat glands of adult humans (Langbein et al. 2005) or in the epidermis of embryonic mice (Bazzi et al. 2007), can be reconciled in that K77 is indeed expressed in both pre- to postnatal eccrine sweat glands but also along with the "classical" epidermal keratins K1 and K10 in suprabasal layers of developing embryonic epidermis of both species. Nonetheless, explicit differences between man and mouse occur with regard to the onset of epidermal K77 expression relative to that of K1 and K10. While in the developing human epidermis, K77 expression begins slightly after that of K1/K10, the opposite with K77/K10 expression before that of K1 is true for mouse epidermis, thus indicating subtle differences between *KRT77* and *KRT1* gene regulatory mechanisms in the two species. More importantly, what renders K77 unique within the keratin family is the observation that the suprabasal epidermal K77 expression completely disappears from human epidermis around birth and is then restricted to sweat gland ducts while this keratin is maintained in the epidermis (including the infundibulum of hair follicles) of adult mice (summarized in Table 1).

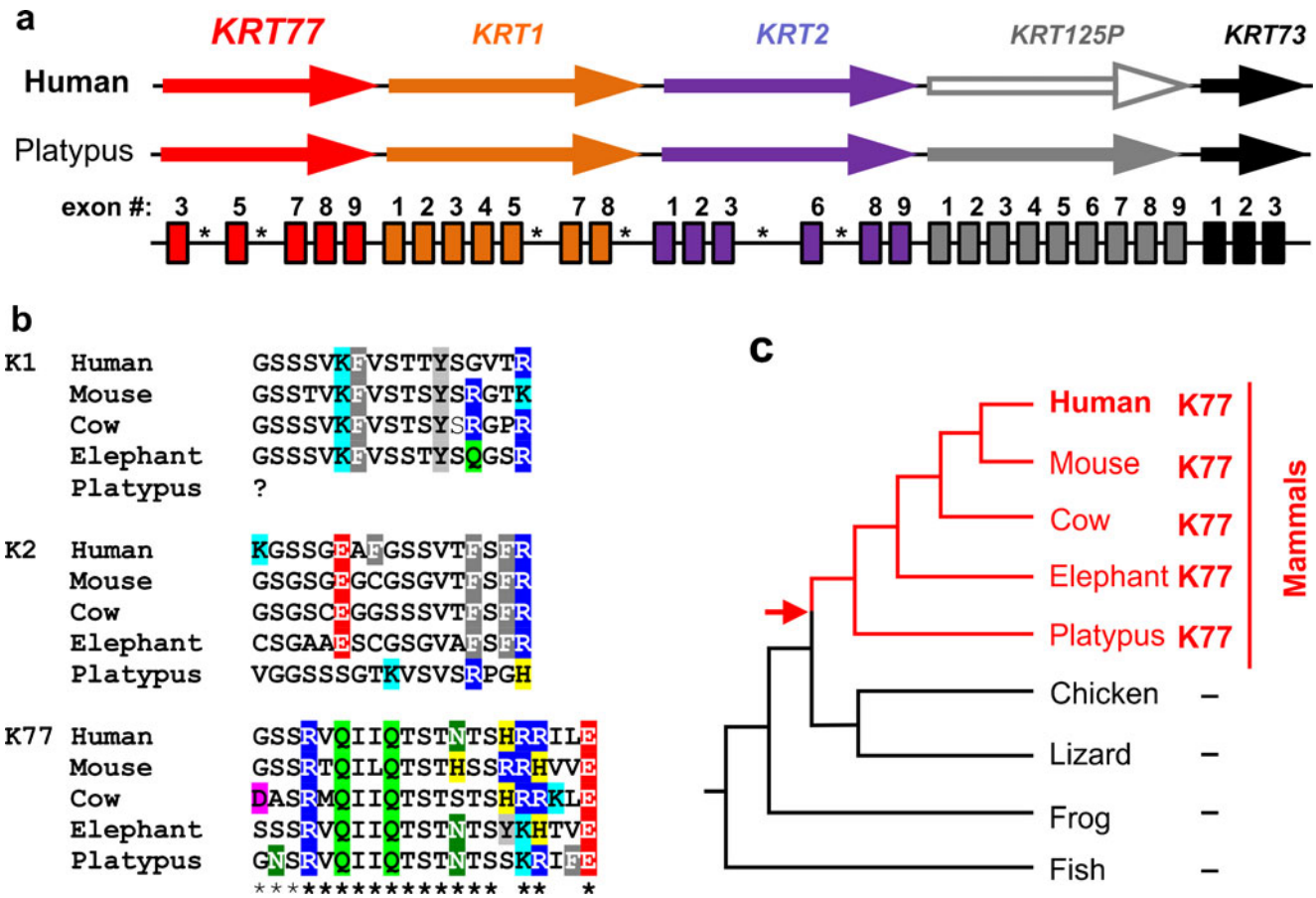

Fig. 8 Evolution of the *KRT77* gene. **a** Comparison of the *KRT77* gene loci in the human genome and in the draft genome of the platypus, which does not include the 5′-end of the *KRT77* gene and contains several sequence gaps (*asterisks*). Platypus exons are indicated by *boxes*. *KRT125P* is a pseudogene in humans, which, in the platypus, is apparently an intact gene at the same position. Note that distances are not drawn to scale. (Annotated genomic sequence of platypus *Krt77* locus is shown in Supplementary Fig. S6). **b** Alignment of the carboxyterminal (*C-terminus*) sequences of K1, K2 and K77 of diverse mammalian species. The C-terminus of platypus K1 is not predictable due to the incomplete draft genome sequence. Amino acids marked by different colors allow for better comparison of sequence motifs. *Asterisks,* conserved/specific sequence motif of K77 with amino acid conservation in at least 3 out of 5 species. **c** Scheme of K77 evolution. Presence or absence of K77 orthologs, as determined by genome sequence screening, was mapped on a phylogenetic tree of representative vertebrates (modified from Eckhart et al. 2008). *Red arrow,* proposed origin of K77 after the divergence (*red lines*) of mammals from sauropsids (including chicken and lizard)

Table 1 Comparison of K77 expression and intracellular distribution patterns in humans and mice

Keratin K77	Human	Mouse
Embryonic epidermis	Suprabasal expression of K77	Suprabasal expression of K77
Adult epidermis	Loss of K77 around birth	Maintenance of suprabasal expression of K77
Eccrine sweat glands	K77 expression in luminal duct cells	K77 expression in luminal duct cells
Keratinocytes in vitro: adherent and organotypic cultures	K77 in differentiated/ suprabasal cells	K77 in differentiated/suprabasal cells
Sequential order of expression	K77 expression subsequent to K1	K77 expression precedes K1
Intracellular localization	Central cytoplasmic concentration of K77 filaments not attached to desmosomes	Conventional cytoplasmic distribution of K77 filaments attached to desmosomes

Remarkably, all but one of the in vivo K77 expression characteristics in embryonic human and mouse epidermis can be observed in adherent and organotypic cultures of epidermal keratinocytes grown under high Ca^{2+} conditions. Even the species-specific differences in the sequential onset of K77 expression relative to that of K1 and K10 in the suprabasal epidermis is retained in both culture systems. What is different, however, to the situation in vivo is that the in vitro differentiation status achieved even under high Ca^{2+} conditions in human cultured keratinocytes or OTCs thereof is not sufficient to eliminate K77 expression. This indicates that the loss of K77 in vivo is closely linked to the fully developed human epidermis, thus precluding the currently available keratinocyte culture systems to be used for investigations on the molecular pathways involved in the loss of K77 from adult human epidermis.

How can these species-specific differences in epidermal K77 expression be explained? Basically, differences at the levels of gene expression (mainly mRNA formation) and post-translational processing (mainly proteolysis) are conceivable. Our data indicate that the total amount of protein within a particular tissue sample correlates with the amount of mRNA, as determined by RT-PCR (Fig. 6) and the loss of mRNA in the adult epidermis as shown by ISH (Supplementary Fig. S2i; Langbein et al. 2005) is accompanied by the loss of this protein (Fig. 2n–q, t-t′; Langbein et al. 2005). Therefore, gene transcription appears to be a critical regulator of K77 abundance and inter-species differences in K77 expression may be attributed to differences in the regulation of *KRT77* versus *Krt77* transcription.

It should be emphasized that K77 is not the only keratin whose expression is timely limited during the embryonic development of the epidermis prior to its expression elsewhere after birth. Related examples are keratins K8 and K18 in the ectoderm (Bader et al. 1988; Jackson et al. 1980; Moll et al. 1982) and K19 in the fetal skin (Gkegkes et al. 2013). Furthermore, the loss of K5/K14 in the keratinocytes of the basal layer during embryonic and adult epidermal differentiation (Coulombe et al. 1989) or K6 and K16, found in embryonic and "activated" epidermal situations such as wounding or pathology (McGowan and Coulombe 1998; Weiss et al. 1984; Paladini et al. 1996; Wong and Coulombe 2003; for review, see also Moll et al. 2008), although in sharp contrast to K77, all of these processes are species-unspecific. As mechanisms of transcriptional control are not known even for these well-established examples of differentially expressed keratins during embryonic skin development, it is difficult to unveil sequence variations that might determine differential K77 expression in the adult epidermis of mouse and man. Regulatory elements of keratin expression have been located not only in the intergenic region upstream of the transcriptional start site (Rothnagel et al. 1993) but also within coding sequences of neighboring keratin genes such as *KRT1b* (now *KRT77*) and *KRT1* (Tao et al. 2006, 2007). This said, future investigation of this open issue will need to be integrated into a study of gene expression at the entire keratin type II locus, in particular that of *KRT1, KRT77* and *KRT2*.

Furthermore, it is conceivable that following the transcriptional silencing of the human *KRT77* gene, residual K77 protein might be removed from adult epidermis by proteasomal degradation via ubiquitinylation. Recently, the E3 ubiquitin ligase, MAFbx has been found to degrade muscular MyoD by binding to an LXXLL core motif (Tintignac et al. 2005). Remarkably, a LEPLL motif is present in linker 1 of the human K77 rod domain (Supplementary Table S2a) but lacks from the corresponding region of virtually all other type II keratins (for examples, see, Supplementary Table S2b). Moreover in addition to man, the critical LEPLL motif occurs exclusively in K77 of primates and hence, is restricted to those species that show postnatal loss of K77 from the epidermis. A comparable developmental switch in the expression of skin-associated differentiation-specific proteins from the epidermis to an adnexal organ has also been observed for murine trichohyalin and the human peroxisome proliferator activated receptors (PPAR) α and -ß (Icre et al. 2006; Lee et al. 1999). Not surprisingly, both contain LXXLL motifs in their penultimate amino- and carboxyterminus, respectively. Further studies on

Table 2 Desmoplakin core binding site in human type II keratins of keratinizing epithelia. Italics, non-conserved motif positions; bold, conserved motif positions

a	**Keratin**	**Binding site**
	K77	*SRSIS*
	K1	S**K**SIS
	K2	T**K**SIS
	K3	N**K**SIS
	K4	N**K**SIS
	K5	S**K**RIS
	K6a	S**K**RIS
	K6b	S**K**RIS
	K6c	S**K**RIS

b	**Species**	**Binding site**
	Human	*SRSIS*
	Chimpanzee	*SRSIS*
	Gorilla	*SRSIS*
	Galago	S**K**SIS
	Mouse	S**K**SIF
	Rat	S**K**SIF
	Horse	S**K**SN

epidermal E3 ligases and the functionality of the binding motif in human K77 are necessary to verify this hypothesis.

A further outstanding feature of K77 is the difference in the appearance of its intracellular IF network in man and mouse. Consistently, keratin IF bundles span through the entire cytoplasm from the nuclear region to the plasma membrane where the filaments attach to the desmosomal plaque via desmoplakin (Kouklis et al. 1994; Meng et al. 1997; Smith and Fuchs 1998). The recently described, ubiquitously expressed keratin K80 was the first member of the family whose IF distribution clearly deviated from this "normal" pattern. K80-containing filaments were strictly located along the inner cell membranes and conspicuously concentrated at sites where other IF bundles spread to attach to the desmosomal plaque (Langbein et al. 2010a). In contrast, the divergence from the "classical" pattern of K77-containing IFs in suprabasal cells of embryonic human epidermis and luminal cells of the eccrine sweat duct consisted in the formation of an IF network that did not abut onto desmosomes but was visibly retracted from them. Conversely, IF bundles built up by the murine K77 displayed the classical way of intracellular organization in suprabasal keratinocytes.

Why does the K77 IF network in human embryonic epidermal cells and luminal duct cells of sweat glands form an empty zone alongside and subjacent to the plasma membrane? It has previously been shown that the binding of human keratin IFs to desmosomes via desmoplakin is mediated by a specific binding core motif GGS**K**S/RIS, which is highly conserved in the non-α-helical head region of type II keratins expressed in keratinizing squamous epithelia (Table 2a; see also Kouklis et al. 1994; Meng et al. 1997; Smith and Fuchs 1998). More precisely, the keratin IF-desmoplakin interaction depends essentially on the lysine residue within the binding motif (Table 2a), as shown by association studies of the carboxy terminal tail domain of desmoplakin with the amino terminal head domain of type II keratins carrying a mutated lysine residue (Kouklis et al. 1994; Meng et al. 1997; Smith and Fuchs 1998). In addition, during terminal differentiation of the epidermis, the lysine residue is also indispensable for the transglutaminase mediated y-glutamyl-lysine cross-linking of keratins to the cornified envelope at the transition of granular cells into corneocytes (Candi et al. 1998; 2005). Therefore the critical lysine residue in type II keratins generally plays a pivotal role in the proper supramolecular organization and function of keratin IFs in epidermal keratinocytes. In the light of these findings, it came as no surprise that keratin K80 lacked the GGSKS/RIS motif altogether (*see* Langbein et al. 2010a) and that the lysine residue in the K77 binding motif was present in the murine keratin but substituted by an arginine residue in the human and primate K77 (Table 2b). In line with this, an IF network displaying a retraction from desmosomes has also been observed in suprabasal epidermal cells of patients suffering from nonepidermolytic palmarplantar keratoderma, NEPPK, caused by a substitution of the critical lysine residue in keratin K1 by isoleucine, although the alterations appeared more subtle due to the heterozygous nature of the substitution, which left half of the IFs with the intact K1 keratin (Kimonis et al. 1994).

In order to deduce the properties and the possible functions of K77 in human and mouse epidermis and sweat gland ducts, it is important to note that, in contrast to the adult human epidermis, K77 expression is maintained in luminal cells into adulthood. Based on the available data, it is evident that the murine keratin K77 fulfils all criteria of a genuine differentiation-specific epidermal type II keratin. Although initially expressed slightly before K1 in parabasal cells, soon after it competes with this keratin for IF formation with K10 and thus makes mouse epidermal differentiation more complex at the keratin level than previously assumed. Similar to keratins K2 and the sole epidermis-specific keratin K9 (Langbein et al. 1993), K77 may also contribute to an enhancement of mechanical stabilization of differentiating epidermal cells. The same holds true for its function in luminal duct cells of eccrine sweat glands in which its additional expression may reinforce the protective role exerted by the compact periluminal keratin belt along the entire lumen against sweat leakage from eccrine sweat gland ducts (Supplementary Fig. S2; Langbein et al. 2005).

Due to the close evolutionary and structural relationship of K77 and K1, it may be speculated that, in case of emergency, the two keratins might be able to substitute each other. Such a phenomenon has previously been reported for the type I hair cortex keratin K41, which during human evolution has been inactivated into a pseudogene and its function in the hair

cortex subsequently been taken over by hair keratin K31 (Winter et al. 2001). Relying on the structurally intact mK77, there is, however, evidence from mice in which the *Krt1* or *Krt1/Krt10* genes have been knocked out (Roth et al. 2012; Wallace et al. 2012) that it cannot substitute for mK1. Remarkably, during the entire embryonic phase, the epidermis of these mice is not only morphologically largely inconspicuous but also exhibits an essentially undisturbed expression pattern of suprabasal mK77 and mK2, or mK10 in the case of the *Krt1*$^{-/-}$ mice (Fig. 7a–b′ and data not shown). However, within hours after birth, vacuolization and blistering develops in the upper spinous and granular layers (Fig. 7c, d, e–f′), resembling the tissue lesions of epidermolytic hyperkeratosis (EH) caused by deleterious mutations in K1 (Kimonis et al. 1994). Interestingly, it has been found that K10-deficient mice, in which the three type II keratins mK1 (Supplementary Fig. S5b, d, f, i), mK77 (Supplementary Fig. S5) and mK2 (Supplementary Fig. S5g, j) are left without their genuine type I partner, survive in that mK1 and mK77 resort to mK14 (Supplementary Fig. S5a, c, e, h; see also Reichelt and Magin 2002; Reichelt et al. 2001, 2004) for IF formation. In contrast, mK1-deficient mice, still containing mK77 and mK2, die shortly after birth (Roth et al. 2012). This shows that, despite their sequence similarity, mK77 is unable to replace mK1 in mouse epidermis.

While there is every reason to believe that mK77 represents a genuine keratin albeit of incompletely understood function, one might expect that the inability of hK77 to bind to desmosomes could transform it into a deleterious keratin. However, like mK77-containing embryonic and adult mouse epidermis and eccrine sweat glands, the hK77-containing embryonic human epidermis and eccrine sweat glands develop normally. Moreover, hK77 is obviously dispensable for the proper function of adult human epidermis. The generation of transgenic mice lacking the *Krt77* gene is one option to precisely define the roles of K77 in vivo further allowing investigations of K77-dependent differences between human and murine skin, in particular in sweat glands.

Acknowledgements This study was supported by the Wilhelm Sander-Stiftung, Munich (Grant 2007.133.2 to L.L.) and in parts by the Newcastle Health Care Charity and the Newcastle upon Tyne Hospitals NHS Charity (Grant PFC/ ML/0809 to J.R.). We thank Hans-Juergen Stark and Iris Martin for normal (NEHK) and immortal (HaCaT) human keratinocytes of adherent and organotypic cultures, Peter Angel for immortalized mouse keratinocytes, Peter Krieg and Sabine Rosenberger for mouse OTCs as well as Hermann Stammer for his support with qPCR and the Core Facility Electron Microscopy for technical equipment (all German Cancer Research Center, Heidelberg, Germany). We are grateful to Marianne Holtkoetter (Wilhelma, Stuttgart, Germany) for providing us with skin of a stillborn gorilla and Ingrid Hausser-Siller (EM-lab Dermatology and EM Core facility, Heidelberg University, Germany) for her invaluable support for our start in ultrathin cryo-sectioning as well as David A. Parry (Palmerston, New Zealand), Rudolf Leube (Aachen, Germany) and Ralf Paus (Luebeck, Germany) for fruitful discussions and Arunima Murgai (Newcastle, UK) for rectifying the English language.

References

Bader BL, Jahn L, Franke WW (1988) Low level expression of cytokeratins 8, 18 and 19 in vascular smooth muscle cells of human umbilical cord and in cultured cells derived therefrom, with an analysis of the chromosomal locus containing the cytokeratin 19 gene. Eur J Cell Biol 47:300–319

Bazzi H, Fantauzzo KA, Richardson GD, Jahoda CAB, Christiano AM (2007) Transcriptional profiling of developing mouse epidermis reveals novel patterns of coordinated gene expression. Dev Dyn 236:961–979

Boehnke K, Mirancea N, Pavesio A, Fusenig NE, Boukamp P, Stark HJ (2007) Effects of fibroblasts and microenvironment on epidermal regeneration and tissue function in long-term skin equivalents. Eur J Cell Biol 86:731–746

Boukamp P, Petrussevska RT, Breitkreutz D, Hornung J, Markham A, Fusenig NE (1988) Normal keratinization in a spontaneously immortalized aneuploid human keratinocyte cell line. J Cell Biol 106:761–771

Byrne C, Hardman M, Nield K (2003) Covering the limb–formation of the integument. J Anat 202:113–123

Candi E, Tarcsa E, Digiovanna JJ, Compton JG, Elias PM, Marekov LN, Steinert PM (1998) A highly conserved lysine residue on the head domain of type II keratins is essential for the attachment of keratin intermediate filaments to the cornified cell envelope through isopeptide crosslinking by transglutaminases. Proc Natl Acad Sci USA 95:2067–2072

Candi E, Schmidt R, Melino G (2005) The cornified envelope: a model of cell death in the skin. Nat Rev Mol Cell Biol 6:328–340

Coulombe PA, Kopan R, Fuchs E (1989) Expression of keratin K14 in the epidermis and hair follicle. Insights into complex programs of differentiation. J Cell Biol 109:2295–2312

Cui CY, Childress V, Piao Y, Michel M, Johnson AA, Kunisada M, Ko MS, Kaestner KH, Marmorstein AD, Schlessinger D (2012) Forkhead transcription factor FoxA1 regulates sweat secretion through Bestrophin 2 anion channel and Na-K-Cl cotransporter 1. Proc Natl Acad Soc USA 109:1199–1203

Durchdewald M, Beyer TA, Johnson DA, Johnson JA, Werner S, Auf dem Keller U (2007) Electrophilic chemicals but not UV irradiation or reactive oxygen species activate Nrf2 in keratinocytes in vitro and in vivo. J Invest Dermatol 127:646–653

Eckhart L, Ballaun C, Hermann M, Vandeberg JL, Sipos W, Uthman A, Fischer H, Tschachler E (2008) Identification of novel mammalian caspases reveals an important role of gene loss in shaping the human caspase repertoire. Mol Biol Evol 25:831–841

Gkegkes ID, Aroni K, Agrogiannis G, Patsouris ES, Konstandinidou AE (2013) Expression of caspase-14 and keratin K19 in the human epidermis and appendages during fetal skin development. Arch Dermatol Res 305:379–397

Groscurth P (2002) Anatomy of sweat glands. Curr Probl Dermatol 30:1–9

Hashimoto K, Gross BG, Lever WF (1966) The ultrastructure of human embryo skin II. The formation of intradermal portion of the eccrine sweat duct and of the secretory segment during the first half of embryonic life. J Invest Dermatol 46:513–529

Hesse M, Zimek A, Weber K, Magin TM (2004) Comprehensive analysis of keratin gene clusters in humans and rodents. Eur J Cell Biol 83:19–26

Heynold H (1874) Über die Knäueldrüsen des Menschen. Arch pathol Anat Physiol Klin Med 61:77–90

Holbrook K (2006) Embryogenesis of the skin. In: Irvine AD, Hoeger PH, Yan AC (eds) Harper's Textbook of pediatric Dermatology, 2nd edn. Blackwell, Oxford , pp 21–241

Holbrook KA, Odland GF (1975) The fine structure of developing human epidermis: light, scanning, and transmission electron microscopy of the periderm. J Invest Dermatol 65:16–38

Icre G, Wahli W, Michalik L (2006) Functions of the peroxisome proliferator-activated receptor (PPAR) α and β in skin homeostasis, epithelial repair, and morphogenesis. J Invest Dermatol 11:30–35

Jackson BW, Grund C, Schmid E, Bürki K, Franke WW, Illmensee K (1980) Formation of cytoskeletal elements during mouse embryogenesis Intermediate filaments of the cytokeratin type and desmosomes in preimplantation embryos. Differentiation 17:161–179

Jave-Suarez LF, Langbein L, Winter H, Schweizer J (2004) Androgen regulation of the human hair follicle: the type I hair keratin hHa7 is a direct target gene in trichocytes. J Invest Dermatol 122:555–564

Kimonis V, DiGiovanna JJ, Yang JM, Doyle SZ, Bale SJ, Compton JG (1994) A mutation in the V1 end domain of keratin 1 in non-epidermolytic palmar-plantar Keratoderma. J Invest Dermatol 103:764–769

Kouklis PD, Hutton E, Fuchs E (1994) Making a connection: direct binding between keratin intermediate filaments and desmosomal proteins. J Cell Biol 127:1049–1060

Kunisada M, Cui CY, Piao Y, Minoru SH, Schlessinger D (2009) Requirement for Shh and Fox family genes at different stages in sweat gland development. Hum Mol Genet 18:1769–1778

Langbein L, Schweizer J (2005) The keratins of the human hair follicle. Internat Rev Cytol 243:1–78

Langbein L, Schweizer J (2013) The keratins of the human hair follicle In: Camacho FM, Tosti A, Price VH, Randall VA, (Eds) Montagna Tricología Enfermedades del folículo pilosebáceo Madrid: Editorial Aula Medica Ed, pp 73–108

Langbein L, Heid HW, Moll I, Franke WW (1993) Molecular characterization of the body site-specific human cytokeratin 9 - cDNA cloning, amino acid sequence and tissue specificity of gene expression. Differentiation 55:57–73

Langbein L, Rogers MA, Praetzel S, Winter H, Schweizer J (2003) K6irs1, K6irs3 and K6irs4 represent the inner root sheath-specific type II epithelial keratins in the human hair follicle. J Invest Dermatol 120:512–522

Langbein L, Spring H, Rogers MA, Praetzel S, Schweizer J (2004) Hair keratins and hair follicle-specific epithelial keratins. Meth Cell Biol 78:413–451

Langbein L, Rogers MA, Praetzel S, Cribier B, Peltre B, Gassler N, Schweizer J (2005) Characterization of a novel human type II epithelial keratin K1b, specifically expressed in eccrine sweat glands. J Invest Dermatol 125:428–444

Langbein L, Rogers MA, Praetzel-Wunder S, Helmke B, Schirmacher P, Schweizer J (2006) K25 (K25irs1), K26 (K25irs2), K27 (K25irs3) and K28 (K25irs4) represent the type I inner root sheath (IRS) keratins of the human hair follicle. J Invest Dermatol 126:2377–2386

Langbein L, Rogers MA, Praetzel-Wunder S, Boeckler D, Schirmacher P, Schweizer J (2007) The novel keratins K39 and K40 are the latest expressed type II hair keratins and complete the human hair keratin family. J Invest Dermatol 127:1532–1535

Langbein L, Eckhart L, Rogers MA, Praetzel-Wunder S, Schweizer J (2010a) Against the rules: human keratin K80 Two functional alternative splice variants, K80 and K80.1, with special cellular localization in a wide range of epithelia. J Biol Chem 285:36909–36921

Langbein L, Yoshida H, Praetzel-Wunder S, Parry DAD, Schweizer J (2010b) The keratins of the human hair medulla: the riddle in the middle. J Invest Dermatol 130:55–73

Lee SC, Lee JB, Kook JP, Seo JJ, Nam KI, Park SS, Kim YP (1999) Expression of differentiation markers during fetal skin development in humans: Immunohistochemical studies on the precursor proteins forming the cornified envelope. J Invest Dermatol 12:882–886

McGowan KM, Coulombe P (1998) Onset of keratin 17 expression coincides with the definition of major epithelial lineages during skin development. J Cell Biol 143:469–486

Meng JJ, Bornslaeger EA, Green KJ, Steinert PM, Ip W (1997) Two-hybrid analysis reveals fundamental differences in direct interactions between desmoplakin and cell type-specific intermediate filaments. J Biol Chem 272:21495–21503

Moll R, Moll I, Wiest W (1982) Changes in the pattern of cytokeratin polypeptides in epidermis and hair follicles during skin development in human fetuses. Differentiation 23:170–178

Moll R, Divo M, Langbein L (2008) The human keratins: biology and pathology. Histochem Cell Biol 129:705–733

Nakamura M, Tokura Y (2009) The localization of label-retaining cells in eccrine gland. J Invest Dermatol 129:2077–2078

Paladini RD, Takahashi K, Bravo NS, Coulombe PA (1996) Onset of re-epithelialization after skin injury correlates with a reorganization of keratin filaments in wound edge keratinocytes: defining a potential role for keratin 16. J Cell Biol 132:381–397

Reichelt J, Magin TM (2002) Hyperproliferation, induction of c-Myc and 14-3-3 sigma, but no cell fragility in keratin-10-null mice. J Cell Sci 115:2639–2650

Reichelt J, Büssow H, Grund C, Magin TM (2001) Formation of a normal epidermis supported by increased stability of keratins 5 and 14 in keratin 10 null mice. Mol Biol Cell 12:1557–1568

Reichelt J, Breiden B, Sandhoff K, Magin TM (2004) Loss of keratin 10 is accompanied by increased sebocyte proliferation and differentiation. Eur J Cell Biol 83:747–759

Riehl A (2009) Identification and characterization of gene regulatory networks controlled by the receptor RAGE in inflammation and cancer. PhD thesis, University of Heidelberg, Germany

Rogers MA, Winter H, Langbein L, Bleiler R, Schweizer J (2004) The human type I keratin gene family: characterization of new hair follicle specific members and evaluation of the chromosome 17q212 gene domain. Differentiation 72:527–540

Rogers MA, Edler L, Winter H, Langbein L, Beckmann I, Schweizer J (2005) Characterization of new members of the human type II keratin gene family and a general evaluation of the keratin gene domain on chromosome 12q1313. J Invest Dermatol 124:536–544

Roth W, Kumar V, Beer HD, Richter M, Wohlenberg C, Reuter U, Thiering S, Staratschek-Jox A, Hofmann A, Kreusch F, Schultze JL, Vogl T, Roth J, Reichelt J, Hausser I, Magin TM (2012) Keratin 1 maintains skin integrity and participates in an inflammatory network in skin through interleukin-18. J Cell Sci 125:5269–5279

Rothnagel JA, Greenhalgh DA, Gagne TA, Longley MA, Roop DR (1993) Identification of a calcium-inducible, epidermal-specific regulatory element in the 3′-flanking region of the human keratin 1 gene. J Invest Dermatol 101:506–513

Schweizer J, Bowden PE, Coulombe PA, Langbein L, Lane EB, Magin TM, Maltheis L, Omary MB, Parry DA, Rogers MA, Wright M (2006) A new consensus nomenclature for mammalian keratins. J Cell Biol 174:169–174

Smith EA, Fuchs E (1998) Defining the interaction between intermediate filaments and desmosomes. J Cell Biol 141:1229–1241

Stark HJ, Willhauck MJ, Mirancea N, Boehnke K, Nord I, Breitkreutz D, Pavesio A, Boukamp P, Fusenig NE (2004) Authentic fibroblast matrix in dermal equivalents normalises epidermal histogenesis and dermo-epidermal junction in organotypic co-culture. Eur J Cell Biol 83:631–645

Stöhr P (1906) Lehrbuch der Histologie und der Mikroskopischen Anatomie des Menschen, 12th edn. G Fischer, Jena, pp 358–359

Tao H, Cox DR, Frazer KA (2006) Allele-specific KRT1 expression is a complex trait. PLoS Genet 2:e93

Tao H, Berno AJ, Cox DR, Frazer KA (2007) In vitro human keratinocyte migration rates are associated with SNPs in the KRT1 interval. PLoS ONE 2:e697

Taylor DK, Bubier JA, Silva KA, Sundberg JP (2012) Development, structure, and keratin expression in C57BL/6J mouse eccrine glands. Vet Pathol 49:146–154

Tintignac LA, Lagirand J, Batonnet S, Sirri V, Leibovitch MP, Leibovitch SA (2005) Degradation of MyoD mediated by the SCF (MAFbx) ubiquitin ligase. J Biol Chem 280:2847–2856

Tokuyasu KT (1989) Use of poly(vinylpyrrolidone) and poly(vinyl alcohol) for cryo-ultramicrotomy. Histochem J 21:163–171

Tokuyasu KT (1997) Immuno-cytochemistry on ultrathin cryosections. In: Spector DL, Goldman RD, Leinwand LA (eds) Cells, alaboratory manual, vol 3, Subcellular localization of genes and their products. Cold Spring Harbour Laboratory, Cold Spring Harbour, pp 1311–13127

Vandebergh W, Bossuyt F (2012) Recurrent functional divergence of early tetrapod keratins in amphibian toe pads and mammalian hair. Mol Biol Evol 29:995–1004

Viallet JP, Dhouailly D (1994) Retinoic acid and mouse skin morphogenesis I. Expression pattern of retinoic acid receptor genes during hair vibrissa follicle, plantar, and nasal gland development. J Invest Dermatol 103:116–121

Wallace L, Roberts-Thompson L, Reichelt J (2012) Deletion of K1/K10 does not impair epidermal stratification but affects desmosomal structure and nuclear integrity. J Cell Science 125:1750–1758

Weiss RA, Eichner R, Sun TT (1984) Monoclonal antibody analysis of keratin expression in epidermal diseases: a 48- and 56-kdalton keratin as molecular markers for hyperproliferative keratinocytes. J Cell Biol 98:1397–1406

Winter H, Langbein L, Praetzel S, Jacobs M, Rogers MA, Leigh IM, Tidman N, Schweizer J (1998) A novel human type II epithelial keratin, K6hf, specifically expressed in the companion layer of the hair follicle. J Invest Dermatol 111:955–962

Winter H, Langbein L, Krawczak M, Cooper DN, Jave-Suarez LF, Rogers MA, Praetzel S, Heidt PJ, Schweizer J (2001) Human type I hair keratin pseudogene ΨhHaA has functional orthologs in the chimpanzee and gorilla: evidence for recent inactivation of the human gene after the Pan-Homo divergence. Hum Genet 108:37–42

Wong P, Coulombe PA (2003) Loss of keratin 6 (K6) proteins reveals a function for intermediate filaments during wound repair. J Cell Biol 163:327–337